Universitätsklinik für Allgemeine, Viszeral- und
Transplantationschirurgie Tübingen

Quality-by-Design Optimization of intraperitoneal Drug Delivery with Pressurized Aerosols

Thesis submitted as requirement to fulfill the degree "Doctor of Philosophy" in *Experimental Medicine* (PhD)

at the Faculty of Medicine Eberhard Karls Universität Tübingen

Presented by:

Sautkin, Iaroslav

2024

Dean: Professor Dr. B. Pichler

1st Reviewer: Professor Dr. U. Lauer
2nd Reviewer: Professor Dr. T. Schäffer

Date of oral defense: 16.01.2024

Table of Contents

List of Abbreviations

ANOVA	analysis of variance
BMI	body mass index
CMA	critical material attribute
CPP	critical process parameter
CQA	critical quality attribute
CRS	cytoreductive surgery
CTCAE	common terminology criteria for adverse events
DAB	3,3′-diaminobenzidine
DAPI	blue-fluorescent DNA stain
DDC	drug-device combination product
DNA	deoxyribonucleic acid
Dx	data distribution
E-charge	electrostatic charge
eIBUB	enhanced inverted bovine urinary bladder
EPIC	early postoperative intraperitoneal chemotherapy
ePIPAC	electrostatic PIPAC
EU	European union
FACS	fluorescence activated cell sorting
FBS	fetal bovine serum
FDA	Food and Drug Administration
FITC	fluorescent reagent for the labeling of amines
FL1	FACS channel

FL2	FACS channel
GLP	good laboratory practice
HIPEC	hyperthermic intraperitoneal chemotherapy
HPLC	high performance liquid chromatography
ICH	International Council for Harmonisation of Technical Requirements for Registration of Pharmaceuticals for Human Use
IDE	investigational device exemption
IHC	immunohistochemistry
IND	investigational new drug
IP	intraperitoneal
IV	intravenous
IVC	intravenous
MAD	median aerodynamic diameter
MDR	Medical Device Regulation
MTT	colorimetric assay for assessing cell metabolic activity
NHDF	normal human dermal fibroblasts
OD	optical density
PBS	phosphate buffered saline
PCI	peritoneal cancer index
PD	pharmacodynamic

PI	cell membrane impermeant dye for the labelling of dead cells
PIPAC	pressurized intraperitoneal aerosol chemotherapy
PK	pharmacokinetic
PM	peritoneal metastasis
PRGS	peritoneal regression grading score
QbD	quality by design
QTPP	quality target product profile
Rpm	revolutions per minute
RT	room temperature
siDNA	signal interfering DNA
siRNA	small interfering RNA

List of Figures

List of Tables

1 Introduction

The peritoneum is subject to metastasis from different origins, with poor prognosis and limited treatment options. Pressurized Intraperitoneal Aerosol Chemotherapy (PIPAC) is aimed to improve the quality of life and patient outcomes. Promising preclinical and clinical results are shown in different entities, especially in patients with unresectable peritoneal metastasis. By adding an electrostatic field to PIPAC (ePIPAC), a shorter application time and more homogeneous drug distribution are expected. In this work, the physical and biological effects of ePIPAC were investigated on a lab stand, in vitro and ex vivo. An optimal application time was proposed based on the highest therapeutic ratio.

1.1 The organ peritoneum

The peritoneum was described in 1836 by Bichat as a two-layer serosae membrane forming a closed

sack. One layer covers the intraabdominal organs and the other one the abdominal wall. Histologically four compounds containing cellular tissue, basement membrane, vessels, and nerves were defined [1]. Although the peritoneum is the second large organ after the skin [2, 3], only minor scientific interest has been shown since 1920 compared to other abdominal organs [4]. Those knowledge gaps in basic and clinical science might affect understanding of the disease, limit their treatment, and hinder patients from becoming a better treatment.

1.1.1 Anatomy

The peritoneum develops from the mesoderm into visceral and parietal layers. The space between two layers is called the abdominal cavity and contains a small volume of fluid. Histologically the peritoneum consists of mesothelial cells on the basal membrane [5]. The gaps between cells form stomata communicating with lymphatic ductules. Lymphatic aggregates around stomata represent "milky spots"

[6]. The parietal peritoneum is vascularised from the abdominal aorta and abdominal wall's arteries [7]. The innervation is by somatic and afferent nerves [8]. The visceral peritoneum is supplied from aa. coeliac, mesenteric superior, and inferior [7] and innervated by the sub-mesothelial autonomous nerve system [8].

1.1.2 Function

The peritoneum has two main functions, the physical ones prevent friction among intraabdominal organs and provide circulation of intraabdominal liquid [1], and the biological ones contribute to wound healing [9], activate an immune response [10, 11] and might prevent infection as well as cancer progression [12, 13].

1.1.3 The peritoneum as a membrane

The peritoneum is a negatively charged [14] semi-permeable membrane [15] with heterogeneous pores, intercellular junctions, lymphatic channels,

and microvilli [16]. The transport through the membrane depends on the substance's nature and molecule size [17, 18]. The small molecules pass through the membrane by diffusion and the large ones by convection [19]. The small pores 4-5nm represent the membrane's intrinsic activity and demonstrate about 95% of the ultrafiltration coefficient. In the large pores (25nm), this coefficient is less than 5%, and in ultra-small ones (0.5nm) is around 1.5% [20].

1.2 Peritoneal metastasis (PM)

The term peritoneal metastasis describes tumor growth within the abdominal cavity involving the peritoneum and intraabdominal organs [21]. Limited PM is a potentially curable disease and therefore, the former term peritoneal carcinomatosis was replaced, where only symptomatic and palliative treatment options were available with no aim to cure [22]. Despite the growing scientific interest, the results are still limited, showing a half-year mean survival.

Furthermore, the growing incidence of PM at higher ages requires more effective and less invasive approaches [23].

1.2.1 Origin and progression

Almost half of the patients suffering from ovarian and pancreatic cancers develop PM in follow-up [24, 25]. Gastric, colorectal, and extra-abdominal malignancies are associated with PM in roughly 10% of cases [26-28]. PM dissemination occurs in two ways: synchronous cell exfoliation from the primary site and metachronous during surgery [29]. Extra-abdominal tumors are characterized by hematogenous or lymphatic spreading [30, 31]. Four stages can be underlined in PM progression: dissemination, adhesion, invasion, and proliferation [13].

1.2.2 Symptoms of PM

In the early stage, PM is asymptomatic, which delays diagnosis [32]. In the majority of the cases,

bowel obstruction and ascites as signs of advanced disease are evident at the first admission. Abdominal pain, fever, weight loss, and low performance can be the symptoms at any stage [33, 34].

1.2.3 Standard of care

The primary treatment of PM is multimodal [35] and contains systemic chemotherapy [36] with only minor benefits [37, 38] and the combination of systemic chemotherapy with CRS and HIPEC [39]. In ovarian cancer, CRS with HIPEC is beneficial [40, 41]. However, the advantages of CRS and HIPEC for other tumors need to be clarified [42-45].

1.2.3.1 Systemic chemotherapy

Randomized clinical studies proved the efficacy of systemic chemotherapy in different malignancies [46-48]. However, in PM, high systemic clearance of hydrophilic agents leads to low concentration in the target tissue [17, 37, 38], resulting in treatment resistance [49-51].

1.2.3.2 Cytoreductive surgery

Cytoreductive surgery is aimed at removing all macroscopic tumor sites [52] to increase survival in selected patients. In the majority of the cases, complete CRS is combined with intraperitoneal chemotherapy [53-56].

1.2.4 Intraperitoneal chemotherapy

Intraperitoneal chemotherapy demonstrates prolonged drug clearance compared to systemic chemotherapy and shows longer tumor exposure [17]. The tissue drug concentration is higher after local chemotherapy with minor systemic toxicity [37, 38, 57]. Early postoperative (EPIC) and hyperthermic intraperitoneal chemotherapies (HIPEC) are most used in clinical practice. EPIC allows intraabdominal chemotherapy utilizing a catheter up to 5 days after surgery [58] but is limited by early adhesions and the risk of catheter-induced infections [59, 60]. HIPEC is predominantly used after complete CRS and presents a combination of

intraabdominal chemotherapy and hyperthermia [61]. Nonetheless, HIPEC is limited by inhomogeneous drug and temperature distribution, low occupational safety, especially in open technique, and long exposure time [62-64].

Significantly increased survival after CRS and HIPEC was reported in the randomized clinical study in ovarian cancer [65]. However, in colorectal cancer, adding HIPEC to CRS showed no benefits. Moreover, a higher complication rate was reported in HIPEC with CRS vs CRS alone [66]. Further clinical trials are required to define HIPEC's role in other malignancies [43-45].

1.3 Pressurized IntraPeritoneal Aerosol Chemotherapy (PIPAC)

PIPAC is an endoscopic procedure applied in PM after diagnostic laparoscopy, calculation of the PCI, and partial peritonectomy or multiple biopsies via the inlying trocars [67]. Therapeutic aerosol showed

superior drug distribution over conventional lavage [68]. With a four times lower drug dosage, PIPAC demonstrated a significantly higher concentration in the visceral peritoneum over HIPEC [69].

1.3.1 Rationale

The physical principles of gas allow homogeneous aerosol distribution within the abdominal cavity [67, 70]. The primary mechanism of drug delivery in the form of aerosol is diffusion or its modification – osmosis [71]. As a result, even hydrophilic substances can move through tissue membranes, and overcome high intratumoral pressure [67, 72].

1.3.2 Technology

PIPAC technology is described elsewhere and requires a spray nozzle Capnopen® (CapnoPen®, Capnomed Ltd, Tübingen, Germany) connected with a high-pressure injector [68]. The therapeutic solution is pressurized through the Capnopen®, leading to aerosol generation. The pressure in the

line varies from 8 to 20 bars [68, 73, 74]. The gaseous part of aerosol is presented by CO_2 insufflated during laparoscopy [68].

1.3.3 Standard operating protocol

PIPAC is a standardized laparoscopic procedure under general anaesthesia utilizing the two-trocars technique. After PM scoring using PCI, described by P. Sugarbaker, ascites evacuation and partial peritonectomy or multiple random biopsies from the different abdominal regions, the Capnopen® is inserted into one of the trocars under laparoscopic control. A syringe with a therapeutic agent is placed into a high-pressure injector and connected with Capnopen® (Figure 1). The injection rate varies from 0.5 to 1.0ml/sec. The operation team leaves the room and initiates aerosolization by remote control. After 30min exposure, an aerosol is released through a closed air waster system, trocars are removed, and wounds are closed [74, 75].

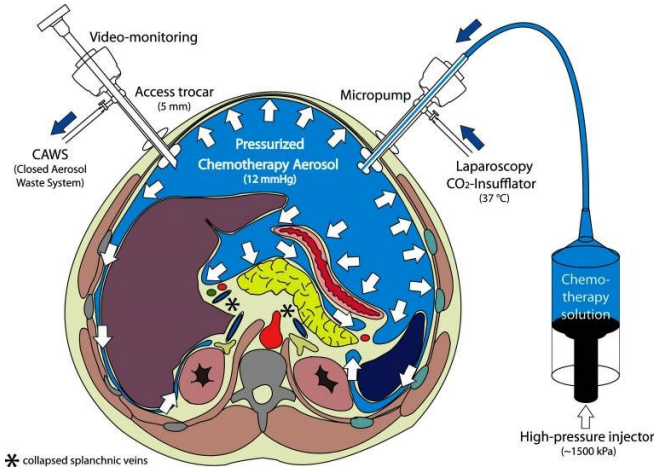

Figure 1. The setup of in human PIPAC [67].

Figure 1 represents the set-up of *in human* PIPAC. On the transverse section of the abdomen, white arrows show the aerosol distribution, and the blue area depicts exposed regions.

1.3.4 Clinical results

In clinical studies, PIPAC has been shown to be safe and well-tolerable, with low systemic toxicity and low clinical adverse events [76, 77]. Encouraging survival was seen in unselected patients with PM

from gastric cancer after different lines of systemic chemotherapy, where PIPAC was aimed to cure [75]. In colorectal, small bowel, and appendiceal PM, an overall survival rate of 10.1 months is described [78]. An adequate histological response of over 70% was reported in ovarian PM [79] and in malignant mesothelioma (histological response of 75%) [80]. A meta-analysis of over 600 patients who underwent PIPAC because of PM from different origins showed an overall histological response of about 40%. After 1400 PIPAC procedures, it was evaluated as safe with meaningful activity against the PM [81]. Hence, PIPAC should be considered as an additional element in a multimodal treatment concept of PM and combined with systemic chemotherapy as well as CRS and HIPEC.

1.3.5 Limitations

There are two limitations reported most often about PIPAC. The first one is inhomogeneous in vivo tissue drug distribution with a significantly higher

drug concentration in the parietal peritoneum over the visceral one [69], and the second one is a reduced drug saturation in the tissue with a higher distance from the spray nozzle [82].

1.4 Electrostatic precipitation Pressurized IntraPeritoneal Aerosol Chemotherapy (ePIPAC)

ePIPAC is the combination of aerosol chemotherapy with electrostatic precipitation aimed to overcome PIPAC limitations [83]. Preclinical and early clinical studies demonstrated safety, applicability, and adequate histological tumor response [69, 83-86]. Enhanced tissue drug uptake and improved distribution were reported [69, 83]. However, the application time remains unclear but might influence tissue drug distribution and, thus, histological response and patient outcome [85, 86].

1.4.1 Rationale

Short high intensive impulses lead to an increase in membrane permeability or electroporation [87]. Reversible electroporation is widely applied in electrochemotherapy to increase tissue drug accessibility [88-90] and tissue drug concentration and improve the homogeneity of drug distribution. As a result, dosage downscaling and a shorter application time might be feasible [83].

1.4.2 Technology

The ePIPAC complements PIPAC, described in 1.3.2, and requires an electrostatic charge generator with two electrodes [83]. The certified class II device from AlesiSurgical® (Ultravision, Alesi Surgical, Cardiff, UK) [91] is in clinical use [85, 92, 93]. The generator is characterized by a current of 1-10μA and a voltage of 7000-10000V. The frequency of the transmitter varies from 150 kHz to 80 MHz [94]. The brush electrode Ionwand® emits negative ions and is inserted intraabdominal. The return plate

electrode has a positive charge and is stuck to the skin [83, 94]. The aerosol becomes negatively charged during spraying and moves under the force of the electrostatic field toward the positively charged abdominal structures [83].

1.4.3 Standard operating protocol

After the PIPAC set-up is completed (see 1.3.3), the Ionwand® electrode is inserted into the abdomen under laparoscopic control. The plate electrode is stuck to the skin [83, 84]. Activation of the electrostatic field follows aerosolization and last from 1 to 30min [84-86]. The exact time is not yet established. The procedure ends with the deactivation of the electrostatic field and the release of the pneumoperitoneum. Both electrodes with trocars are removed and the wound is closed [84].

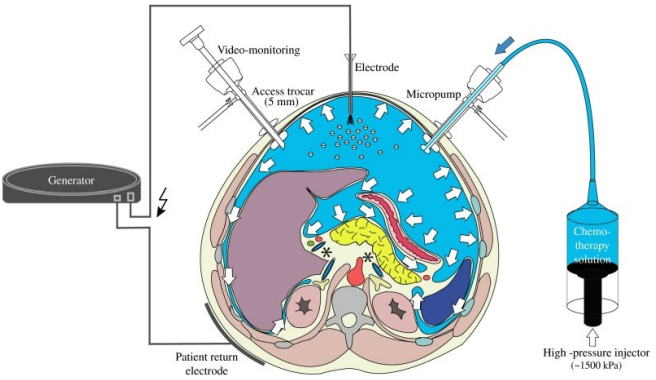

Figure 2. ePIPAC setup.

The electrode is introduced intraabdominally through the wall, and the patient's return electrode is stuck to the skin. Both electrodes were connected to the generator [83].

Figure 2 describes the set-up of ePIPAC. The position of Ionwand® ("Electrode" on the picture) and return plate electrodes are shown on the cross-section of the human abdominal cavity. The aerosol distribution is indicated with white arrows, and a blue field depicts the area exposed to the aerosol [83].

1.4.4 Clinical results

Despite the limited clinical experience, ePIPAC is demonstrated to be safe and applicable [85, 86]. The high systemic drug bioavailability is comparable with systemic administration [93]. However, an optimal application time is not yet established [84, 86]. After one minute ePIPAC, a histological response of 60% was reported [85], and Phase II clinical trials on colorectal PM are currently ongoing [92, 95].

1.5 Knowledge gaps

- PIPAC has an inhomogeneous intraabdominal drug distribution

After PIPAC in swine, drug concentration was considerably lower in the visceral peritoneum than in the parietal one. However, the same difference was observed after HIPEC [64, 69]. These results allow assuming that drug delivery is conditioned not only by the drug-device system but also by targeted organs.

- ePIPAC is used with no proper pharmacological data

There is no data showing overtime tissue drug distribution during ePIPAC. Over time systemic toxicity and tissue drug clearance were not investigated so far.

- No comprehensive comparison of ePIPAC vs PIPAC

The following parameters should be compared: real-time tissue aerosol absorption and sedimentation; systemic toxicity and drug clearance; over time tissue drug distribution.

- The optimal application time is unknown

Application time in ePIPAC varies from 1 to 30min [84-86]. No data demonstrate the optimal application. It is not established when the electrostatic charge should be activated during aerosolization or after.

1.6 Hypotheses

1.6.1 ePIPAC is superior to PIPAC

Electrostatic precipitation modifies the pharmacological and biological effects of PIPAC. An application time is expected to be shorter.

1.6.2 Better therapeutic index (IP/IV)

Applying the same dosage of doxorubicin, higher tissue drug availability is expected after ePIPAC vs PIPAC.

1.6.3 Shorter delivery time

ePIPAC can shorten PIPAC.

1.6.4 Deeper tissue penetration

Doxorubicin penetration is expected to be the same as in PIPAC.

1.6.5 Higher tissue concentration

Doxorubicin tissue concentration is expected to be the same as in PIPAC.

1.6.6 Better homogeneity

Doxorubicin concentration and depth of penetration among and within visceral and parietal organs will be more homogeneous after ePIPAC than after PIPAC.

1.6.7 Enhanced biological effect(s)

Local drug toxicity is expected to be higher in ePIPAC vs PIPAC.

2 Materials and Methods

The target effect of drug delivery systems such as PIPAC or ePIPAC is mainly caused by a therapeutic substance. Thus, technological optimization and evaluation of its treatment effect are not possible without consideration of applied drugs.

Whereas the evaluation of (e)PIPAC as a drug-device combination might appear self-evident, we have rapidly found that this is not the case. The challenges encountered can be classified into three categories:

- The regulatory requirements

European Medicine Agency defines a Drug-Device Combination Product (DDC) as a medicinal product(s) with integral and/or non-integral medical device/device component(s) necessary for administration, correct dosing, or use of the medicinal product [96]. According to regulatory

advice [97], the Capnopen® device is appropriately classified as a Class IIB medical device according to European Medical Devices Regulation (MDR) [98]. In contrast, the US Food and Drug Administration (FDA) considers PIPAC a class III (high-risk) drug-device combination, requiring both an Investigational Device Exemption (IDE) and an Investigational New Drug (IND) approval for starting clinical studies in humans. The regulatory documents, in particular:

- The generic nature of (e)PIPAC as a drug delivery system

Pressurized Intra Peritoneal Aerosol Chemotherapy (PIPAC) is a generic drug delivery technique that distributes an extensive, heterogeneous range of therapeutic substances. These include small molecule drugs, targeted agents (antibodies), nanomolecules, genes (siDNA, siRNA), and cytolytic viruses.

- The complexity of the system under study

Table 1. Parameters influencing transmesothelial drug transport [99].

Therapy-related	Drug-related	Tumor tissue related
Dose	Molecular weight	Permeability
Temperature	Ionic charge	Vascularity
Carrier fluid	Membrane binding	Interstitial fluid pressure
Volume of carrier fluid	Solubility	Cell density
Intra-abdominal agents	Diffusivity	Extracellular matrix composition
Surface use		
Duration		

Three groups of parameters influence the transmesothelial drug transport during intraabdominal chemotherapy: therapy-related, drug-related, and tumor tissue related.

2.1 Quality by design approach

Exploring all theoretical drug-device combinations experimentally under all possible physicochemical

environmental conditions appears sheerly impossible.

FDA encourages risk-based approaches and the adoption of "Quality by design" (QbD) principles in drug product development, manufacturing, and regulation [100]. ICH defines QbD as a systematic approach to development that begins with predefined objectives and emphasizes product and process understanding and process control based on science and quality risk management [101]. QbD is a systematic scientific and risk-based approach to pharmaceutical manufacturing where quality is built-in through product and process understanding [102].

QbD elements are summarised in the following table (adapted from [103]).

Table 2. Quality by design: elements and definitions according to ICH Q8.

QbD element	Definition	Addressed in this study
Quality target product profile (QTPP)	A prospective summary of the quality characteristics of a drug product that ideally will be achieved to ensure the desired quality, taking into account safety and efficacy	Yes
Critical quality attributes (CQAs)	A physical, chemical, biological, or microbiological property or characteristic that should be within an appropriate limit, range, or distribution to ensure the desired product quality	Yes
Critical material attributes (CMAs)	A physical, chemical, biological, or microbiological property or characteristic of an input material that	Yes

	should be within an appropriate limit, range, or distribution to ensure the desired quality of output material.	
Risk assessments	A systematic process designed to coordinate, facilitate and improve science-based decision-making concerning the benefit/risk ratio	Yes
Design space	The multidimensional combination and interaction of input variables (e.g., material attributes) and process parameters have been demonstrated to assure quality	Yes
Critical process parameters (CPPs)	A process parameter whose variability has an impact on a CQA and, therefore, should be monitored or controlled to ensure the process produces the desired quality	No

Control strategy	An alternative approach to process validation in which manufacturing process performance is continuously monitored and evaluated	No
Lifecycle management	All phases in the life of a product, from the initial development through marketing until the product's discontinuation.	No

2.2 Study design

According to FDA guidance for QbD, a Formal Experimental Design (also known as "Design of Experiments.") has to be determined prospectively as a structured, organized method for determining the relationship between factors affecting a process and the output of that process.

This experimental study investigated the influence of electrostatic precipitation on drug uptake into the peritoneal tissue during PIPAC.

Several dimensions were addressed, including tissue drug concentration, depth of drug tissue penetration, homogeneity of spatial drug distribution, local toxicity, and aerosol size distribution. An additional, clinically relevant dimension was to determine the minimal exposition time needed to apply a drug efficiently into the peritoneal tissue.

The study was designed in three successive steps:

1. Physical experiments were performed on a lab stand to understand the behaviour of the therapeutic aerosol over time,
2. Pharmacological experiments were performed ex vivo to determine tissue drug uptake,
3. Biological experiments were performed in vitro and ex vivo.

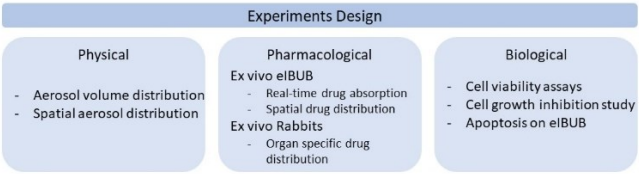

Figure 3. Experiments design.

This figure demonstrates experiments performed. There are three groups physical, pharmacological, and biological experiments. Physical one explains the aerosol behaviour over time, pharmacological – tissue drug distribution, and biological – local toxicity.

Physical differences between PIPAC and ePIPAC were investigated on the lab stand, biological and pharmacological on in vitro and ex vivo models. All experiments were in triplicate.

2.3 Ethical and regulatory framework

According to German law, no ethical approval was needed for physical, in vitro, and ex vivo experiments. No animals were sacrificed for scientific purposes.

2.4 Safety Regulations and occupational health safety

All experiments were performed in the lab of the National Centre for Study of Pleura and Peritoneum. Manipulation with the cytotoxic drugs was in the approved exhaust hood, and protective clothes were put on. All wastes were disposed of according to German regulations by the internal clinic service. Air and surface contaminations with cytotoxic drugs are regularly checked.

2.5 Models used

Six models were applied. Physical experiments were on "Overtime aerosol sedimentation model" and "2D and 3D blotting paper"; in vitro experiments on "2D cell culture" and "electrostatic cell culture model"; ex vivo on "enhanced inverted bovine urinary bladder" and on "rabbit model".

2.5.1 Overtime aerosol sedimentation model

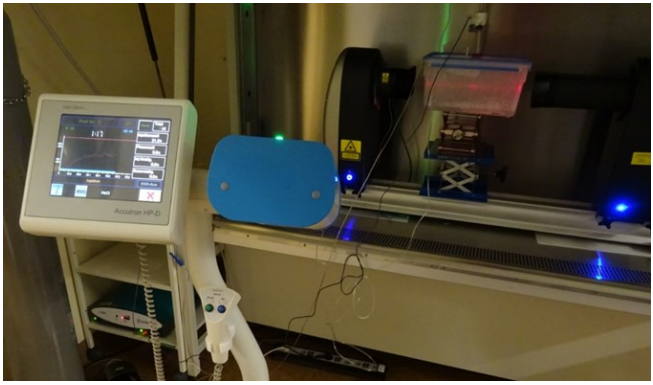

Figure 4. Model setup for overtime granulometry during ePIPAC.

Aerosol was distributed within a given space during PIPAC and ePIPAC. Over time MAD and transmission were measured by laser diffraction.

2.5.2 2D and 3D blotting paper model

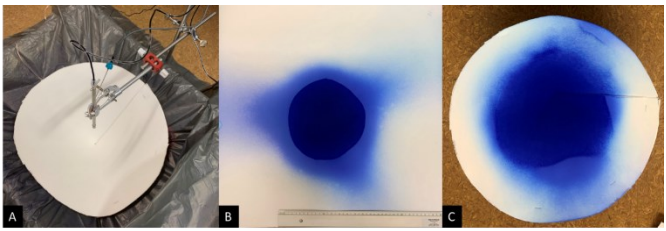

Figure 5. 2D and 3D blotting paper model.

A: The model setup; B: 2D (planar) distribution; C: 3D (volumetric) distribution.

The spray patterns after PIPAC and ePIPAC were explored on 2D and 3D blotting paper. A portion of blue ink was aerosolized with Capnopen® over blotting paper following photo documentation and results quantification.

2.5.3 In vitro experiments

Immortal normal human dermal fibroblasts were plated for viability and growth inhibition studies. Apoptotic cells were labelled with annexin V/PI and counted by FACS and fluorescence microscopy. MTT demonstrated relative cell viability after

PIPAC and ePIPAC. Cell growth inhibition was confirmed by regular cell count with a CASY® cell counter.

2.5.4 Electrostatic cell culture model

For ePIPAC on cell culture, the electrostatic cell culture model was invented.

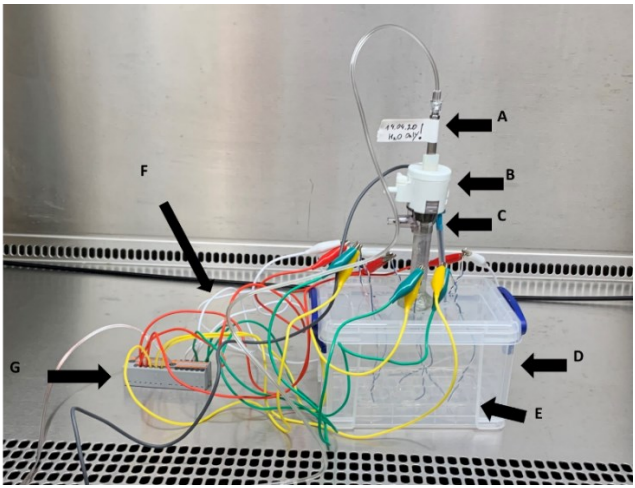

Figure 6. The setup of the electrostatic cell culture model.

A - CapnoPen® spray nozzle, B - 12-mm trocar, C - active brush electrode, D - plastic box, E - cell culture plate, F - return electrodes, and G - splitter.

A cell culture plate was placed in the airtight plastic box. The negative electrode was at the top of the box, and the positive electrodes were on the surface of each well. Capnopen® was inserted through the trocar (see Figure 6). The applicability and reproducibility of the model were proven on 2D cell cultures and 3D grafts.

2.5.5 Enhanced Inverted Bovine Urinary Badder (eIBUB)

The application time of ePIPAC was optimized on eIBUB. The model comprises an inverted bovine urinary bladder connected with an airtight plastic cup by the principle of communicating vessels.

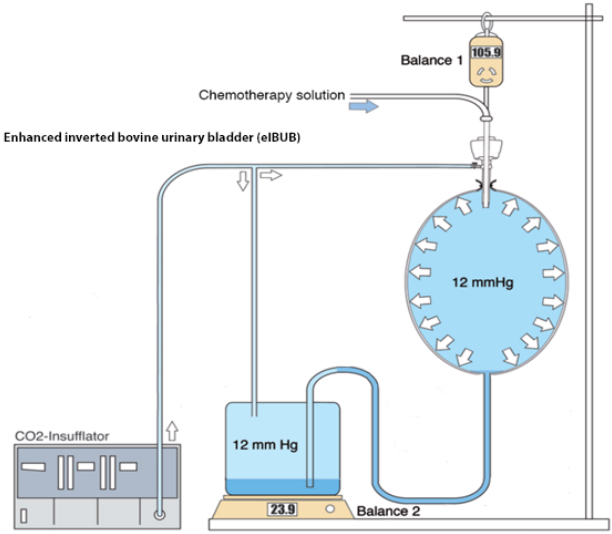

Figure 7. The setup of the enhanced inverted bovine urinary bladder (eIBUB).

Based on the described model, real-time tissue aerosol absorption and aerosol sedimentation were measured, as well as spatial drug distribution. The model is suitable for the optimization of drug-delivery systems and medicaments.

2.5.6 Large animal model

Ex vivo rabbit model

Doxorubicin distribution between intraabdominal organs was compared after PIPAC vs ePIPAC in the cadaveric rabbit model. However, no PK/PD and toxicity were possible. The influence of drug clearance on local tissue drug concentration remained unclear.

2.6 Drugs used

Doxorubicin and cisplatin were used in this study. Spatial distribution was investigated by the depth of doxorubicin penetration and tissue concentration of both drugs. In vitro and ex vivo local drug toxicity was measured.

2.6.1 Choice of drugs

Doxorubicin and cisplatin are the most often off-label drugs applied *in human* PIPAC and ePIPAC. Doxorubicin is a red powder soluble in water, positively charged in physiological pH, and belongs

to anthracycline antibiotics. Antitumor activity due to intercalation into DNA causes replication abruption. Indications: gynaecological and abdominal malignancies.

Cisplatin is a solid yellow powder soluble in water and has a neutral charge. Traditionally, it belongs to alkylating agents — the antitumor activity due to cross-linking the DNA strengths causing replication and proliferation disturbance. Indications: testicular, ovarian, and bladder cancers.

2.6.2 Safety regulation and occupational health safety

Manipulation with doxorubicin and cisplatin was performed in the laboratory under the certified exhaust hood Maxisafe 2020® (Thermo Electron LED Ltd, Langenselbold, Germany) approved for cytotoxics. Protective clothes were put on. All wastes were disposed of in consent with German regulations by the internal clinical service.

2.6.3 Drug Preparation

Doxorubicin Doxo-Cell® 2mg/ml (Cell Pharm® Ltd, Bad Vilbel, Germany) and cisplatin Teva® 1mg/ml (Teva® Ltd, Ulm, Germany) were purchased from the university pharmacy and prepared for aerosolization in our lab.

In ex vivo studies, doxorubicin 1.35ml diluted in 48.65ml 0.9% NaCl and cisplatin 13.5ml diluted in 136.5ml 0.9% NaCl were pipetted separately into two 200ml Medtron® syringes (Medtron® AG, Saarbrücken, Germany) and tightly closed. The final dosage of doxorubicin was 2.7mg and cisplatin 13.5mg.

For in vitro studies, doxorubicin 675µl and cisplatin 6750µl were diluted in 92.575ml of 0.9% NaCl and pipetted into a 200ml Medtron® syringe. The final concentration of doxorubicin was 2.49×10^{-5} mol/L and cisplatin 2.25×10^{-4} mol/L.

2.6.4 Drug application

Ex vivo and in vitro experiments were conducted in the laboratory in the certified exhaust hood Maxisafe 2020®.

Solutions were aerosolized with certified spray nozzle Capnopen® (Capnomed, Zimmern, Germany) connected to injector Accutron HP-D® (Medtron® AG, Saarbrücken, Germany).

2.7 Physical experiments

Aerosol sedimentation during ePIPAC and PIPAC was measured by laser diffraction. MAD and transmission were recorded in triplicate.

Spray patterns were defined after ePIPAC and PIPAC with blue ink on 2D and 3D blotting paper. Experiments were in triplicate.

Hypothesis$_0$: There are no differences in aerosol sedimentation and spatial ink distribution after ePIPAC vs PIPAC.

2.7.1 Real-time aerosol sedimentation

Aerosol sedimentation was measured by the Malvern Spraytec® during ePIPAC and PIPAC. A plastic box with two holes on the sides was placed on a laser beam track in a way that the laser could radiate undisturbed through the holes.

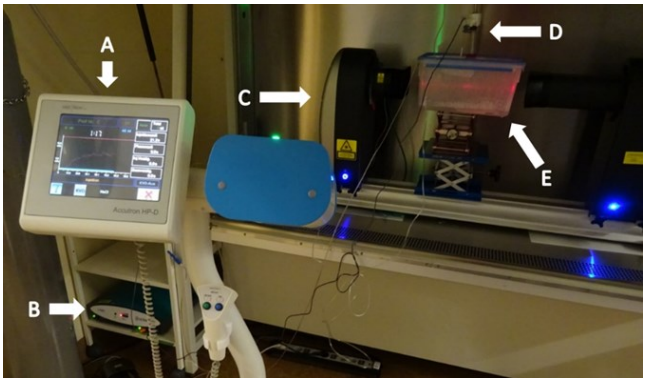

Figure 8. Model setup for overtime granulometry during ePIPAC and PIPAC.

A – high-pressure injector Accutron-HP; B – electrostatic charge generator Ultravision; C – laser diffraction system Spraytec; D – trocar with inserted spray nozzle Capnopen®; E – plastic box.

The Capnopen® was inserted into the trocar at the top of the plastic box and connected to a syringe with

0.9% NaCl loaded to the injector Accutron HP-D®. The laser was turned on, and 60ml of NaCl was aerosolized with 0.7 ml/sec following 10min exposure. During the experiment, MAD and laser transmission were instantly recorded. For ePIPAC, an electrostatic field generator with two electrodes was applied. The first electrode was placed at the top of the box and the second one on the bottom. The device was turned on at two different time points. In the first group, after aerosolization, and in the second group, at the beginning of aerosolization. The device was turned off at the end of the 10min exposure time in both groups. An experiment was terminated earlier if no signal from the laser was detected. All measurements were in triplicate.

2.7.2 Spray patterns: 2D and 3D

The piece of blotting paper 50 x 50 cm was placed in the plastic box, and the Capnopen® in the center of the paper, 10cm above the surface. The syringe was filled with blue ink, loaded to the injector

Accutron HP-D® and connected with the Capnopen® through a high-pressure line. The spray parameters were set up to an injection flow of 0.6ml/sec and a solution volume of 20ml. The spray device and blotting paper were covered with a film, to prevent surface contamination, following aerosolization. For 3D experiments, a conical folded piece of blotting paper was implemented with the same settings described above. The spray device was placed at a level of cone base. For ePIPAC, blotting paper was sprayed with water, and a generator of an electrostatic field with two electrodes was implemented. One electrode was connected to Capnopen®, and another one was stuck to the blotting paper from the outer side. The generator was activated from the beginning of aerosolization until the end of the experiment.

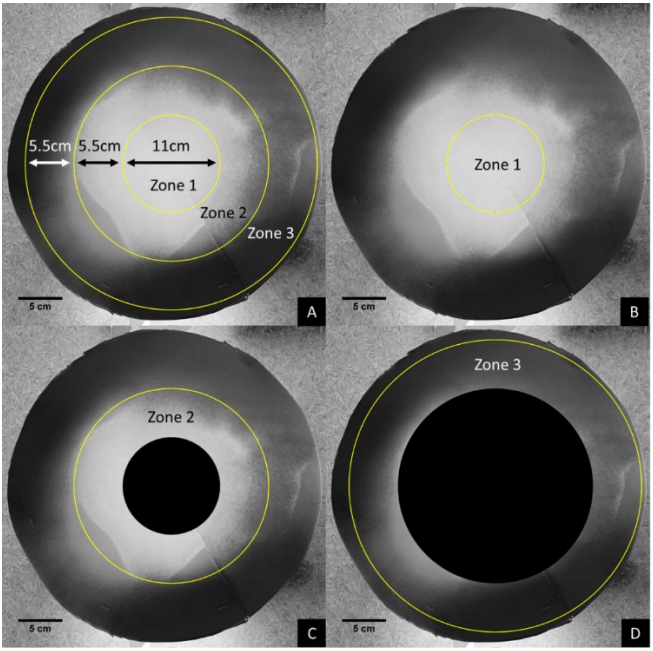

Figure 9. Analysis of spatial ink distribution after ePIPAC vs PIPAC on 3D blotting paper.

A: size of zones; B: measurement in zone 1; C: measurement in zone 2; D: measurement in zone 3. The black circle shows excluded part.

The results were quantified with ImageJ®. Photos were converted to 8-bit and inverted. Ink distribution was analyzed in three zones. In 2D, the first two zones were round 20cm and 40cm in diameter, and

the third one was a rectangle of 50 x 50cm. In 3D, zones were round with a diameter of 11cm, 22cm, and 33cm. All zones were centered. The measurements were from smaller to larger zones, excluding the surface of the smaller ones from the larger ones. Mean intensity and integrated density were calculated and compared among zones and procedures.

2.8 In vitro experiments

2.8.1 Study design

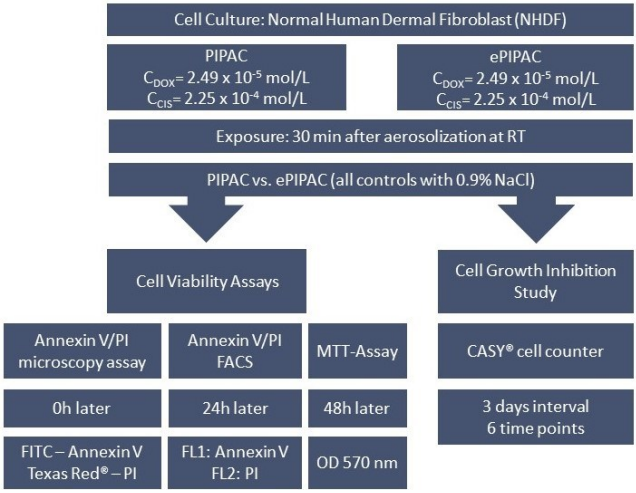

Figure 10. Study design. In vitro ePIPAC vs PIPAC.

In vitro ePIPAC vs PIPAC comprises two parts: cell viability assays and cell growth inhibition study. Experiments were performed with immortal normal human dermal fibroblasts. Test groups underwent PIPAC and ePIPAC with doxorubicin 2.49x10^{-5} mol/L and cisplatin 2.25x10^{-4} mol/L, and controls with 0.9% NaCl.

Hypothesis$_0$: There is no difference in cell viability and cell growth after ePIPAC vs PIPAC.

Additionally, apoptosis conditioned by cleaved caspase-3 was qualitatively and quantitatively analyzed after ePIPAC vs PIPAC on eIBUB.

Hypothesis$_0$: There is no qualitative and quantitative difference in cleaved caspase-3 after ePIPAC vs PIPAC.

2.8.2 Cell line

Immortal normal human dermal fibroblasts have the same histological features as human fibroblasts in the submesothelial connective tissue or scars after cytoreductive surgery. The "immortal" nature of cells and high proliferation rate demonstrate similarity with tumors and allow long-term experiments over different passages.

2.8.3 Cell viability assays

Cell viability as a response parameter to chemotherapy was investigated at different times after therapy with Annexin V/PI microscopic assay at T=0h, FACS Annexin V/PI at T=24h, and MTT assay at T=48h.

2.8.4 Annexin V/PI microscopy assays

NHDF were cultured on six 8-well chamber slides at the density of $3x10^4$ cells/well and viability over 90%. One chamber slide per group, four groups: ePIPAC, PIPAC, positive and negative controls. 72h later, 90% cell confluence was confirmed, the medium was aspirated, and the cells were washed with PBS. The chamber slide was placed in an airtight plastic box on top of which the spray nozzle Capnopen® was inserted. In the ePIPAC group, two electrodes were also placed — one at the top of the box and another on the well's surface.

A syringe with doxorubicin and cisplatin / 0.9% NaCl was loaded into the injector Accutron HP-D®, and connected with the Capnopen® through a high-pressure line. In the ePIPAC group, the electrostatic field generator was turned on following aerosolization of 20ml cytostatics / NaCl — 30min exposure time at RT. Positive control was incubated with 150µM etoposide for 6h.

Immediately after experiments (0h exposure time), cells were twice washed with cold PBS and once with an annexin binding buffer. Annexin V/PI solution was added for 15min in the dark at RT. Cells were washed with annexin binding buffer, and 4% formalin was added for 10min in the dark at RT. Cells were twice washed with annexin binding buffer following incubation with DAPI for 5min in the dark at RT. Cells were twice washed with annexin binding buffer, and the surface was covered with annexin binding buffer. Microscopy was performed with FITC, Texas Red®, and DAPI

filters, 20x magnification under the motorized microscope (Zeiss® Axio Observer, Carl Zeiss Microscopy Ltd, Jena, Deutschland). Field overview with light microscopy. Twenty pictures per group were taken for qualitative and quantitative analyses.

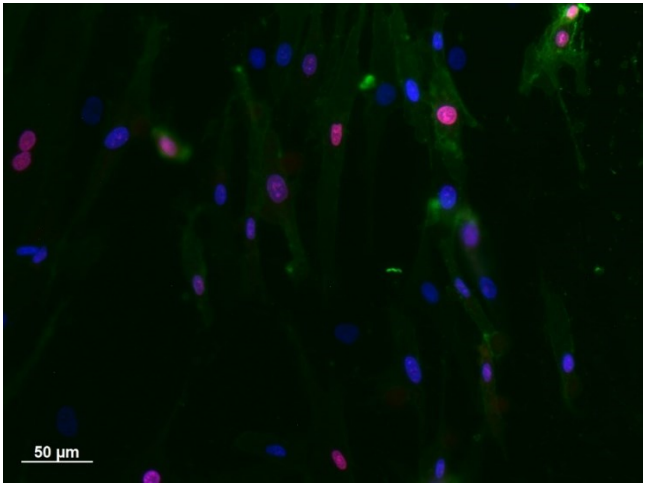

Figure 11. Apoptosis by Annexin V/PI fluorescence microscopy.

An example of apoptosis assay after ePIPAC. Blue nuclei staining with no hollow – alive cells; blue nuclei with green hollow – early apoptosis; rose nuclei with a green hollow – late apoptosis; rose nuclei with no hollow – dead cells.

2.8.5 Annexin V/PI FACS

NHDF were seeded on 22 100mm-Petri dishes at the density of $3x10^4$ cells/dish and cell viability over 90%. There were three dishes for the PIPAC test and PIPAC control, three for the ePIPAC test and ePIPAC control, three for the negative control, and five for the positive control, two dishes as a reserve. 72h later medium was changed, and 144h after cell seeding experiments were performed. The medium was aspirated, and cells were washed with PBS. The Petri dish was placed in an airtight plastic box on top of which the spray nozzle Capnopen® was inserted. In the ePIPAC group, two electrodes were also placed — one at the top of the box and another on the Petri dish's surface.

A syringe with doxorubicin and cisplatin / 0.9% NaCl was loaded into the injector Accutron HP-D®, and Capnopen® was connected with the syringe through a high-pressure line. In the ePIPAC group, the electrostatic field generator was turned on

following aerosolization of 20ml cytostatics / NaCl — 30min exposure time at RT. Cytostatics / 0.9% NaCl were aspirated and 12ml medium with 10% FBS were added. The positive control was incubated with 150µM etoposide for 6h. 24h later, Annexin V/PI FACS was conducted.

On the day of FACS, the medium was aspirated to the 50ml Eppendorf, cells were washed with PBS, and aspirate was collected to the same Eppendorf. 3ml of trypsin was added per dish for 8min in an incubator. The cell suspension was aspirated to the same Eppendorf, and the medium was added to 50ml following centrifugation for 10min at 1500rpm. The supernatant was aspirated, and the cell pellet was resuspended in 15ml PBS. The cell number was normalized between Eppendorf tubes following centrifugation for 10min at 1500rpm. The cell pellet was resuspended in 1ml of annexin binding buffer, and 100µl was transferred to the FACS tube. 5µl of Annexin V and 10µl of PI were added per FACS

tube with 15 min incubation at RT in the dark. FACS within 60min after cell labelling.

FACS was conducted with two channels, FL1: Annexin V and FL2: PI, with the number of events $1x10^4$. Before analysis, channels were gated with positive control stained with Annexin V, positive control stained with PI, unstained positive and negative controls, positive and negative controls stained with Annexin V and PI.

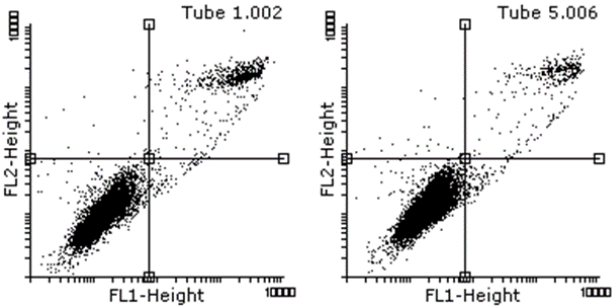

Figure 12. AnnexinV/PI FACS.

Tube 1.002 – PIPAC and Tube 5.006 – ePIPAC test groups. FL2 on y-axis – PI and FL1 on x-axis – annexin V.

2.8.6 MTT-Assays

NHDF were seeded on six 6-well plates at the density of $4x10^4$ cells/well and cell viability over 90%. Two plates for test groups, two for controls, one as a general untreated control, and one plate as a reserve. One blank plate with a solubilizing solution as a negative control. 72h later, the medium was changed with no FBS. The next day ePIPAC and PIPAC were in test and control groups. The medium was aspirated, and cells were washed with PBS. The culture plate was placed into an airtight plastic box on top of which the spray nozzle Capnopen® was inserted. In the ePIPAC group, two electrodes were also placed — one at the top of the box and another split in 6 and placed on the surface of each well.

A syringe with doxorubicin and cisplatin / 0.9% NaCl was loaded into the injector Accutron HP-D®, and Capnopen® was connected with the syringe through a high-pressure line. In the ePIPAC group,

the electrostatic field generator was turned on following aerosolization of 20ml cytostatics / NaCl — 30min exposure time at RT. Cytostatics / NaCl was aspirated, and 2ml of medium with 10% FBS per well was added. MTT-assays in 48h. Biological controls in triplicate with different passages.

On the day of the MTT-Assays, the medium was aspirated, cells were washed with PBS, and MTT solution was added for 4h at 37º C. MTT solution was aspirated, and the solubilizing solution was added for 30min at RT shaking at 100rpm. From each well, 200µl were pipetted into a 96-well plate in triplicate, and light absorption at OD 570nm was measured by colorimetry. Cell viability was calculated by the equation:

$$(\text{mean OD test or control} - \text{mean OD blank}) / (\text{mean OD general control} - \text{mean OD blank}) \times 100$$

2.8.7 Cell Growth Inhibition Study

NHDF were cultured on four 6-well plates at density $4x10^4$ cells/well and viability over 90%. Cell count 96h after seeding, the medium was changed with no FBS. The next day ePIPAC and PIPAC in test/control groups were performed, one plate per group. The medium was aspirated, and cells were washed with PBS. The culture plate was placed into an airtight plastic box on top of which the spray nozzle Capnopen® was inserted. In the ePIPAC group, two electrodes were also placed — one at the top of the box and another was split into 6 and placed on the surface of each well.

A syringe with doxorubicin and cisplatin / 0.9% NaCl was loaded into the injector Accutron HP-D®, and Capnopen® was connected with the syringe through a high-pressure line. In the ePIPAC group, the electrostatic field generator was turned on following aerosolization of 20ml cytostatics / NaCl — 30min exposure time at RT. Cytostatics / NaCl

was aspirated, and 2 ml of medium with 10% FBS per well was added. Cell count and medium change every 72h, six times. Biological controls in triplicate with different passages.

2.8.8 Apoptosis qualitative Analysis

Apoptosis caused by cleaved caspase-3 was qualitatively analyzed after ePIPAC vs. PIPAC on the eIBUB model. Three groups of three bladders were assigned for each procedure, including negative control. Three biopsies from the middle of each bladder were taken after the experiment.

The setup of ePIPAC and PIPAC on the eIBUB model is described in chapters 2.5.5 and 2.9.2. After doxorubicin and cisplatin aerosolization, an exposure time was 30min following tissue sampling and embedding into paraffin blocks. In ePIPAC, an electrostatic field was activated during the whole experiment, and in the control group, no treatment was performed.

Paraffin blocks were half sliced on a microtome. Six 5µm sections per biopsy, three for analysis and three as a technical control were mounted onto a microscope slide and airdried overnight. The following day sections were deparaffinized in xylene and rehydrated in ethanol. Consequently, slides were dipped into a 0.05M Tris buffer for 60min, 3% peroxide buffer for 3min, and again into 0.05M Tris buffer for 3min. Antigen retrieval began by heating slides in 0.01M citrate buffer at 80-100ºC for 15min and after cooling at RT, immersing into a saline buffer. For antigen detection, unspecific signals were blocked with 1% goat serum for 20min. The goat serum was removed, and primary antibodies were added for 60min. In technical controls, primary antibodies were replaced by a saline buffer. Sections were twice washed with 0.05M Tris buffer for 5min. Secondary biotinylated goat anti-rabbit antibodies were added for 10min. Sections were washed with 0.05M Tris buffer and

incubated with streptavidin peroxidase for 5min. Sections were washed with 0.05M Tris buffer, and DAB solution was added for 8min. The slides were counterstained with hematoxylin and eosin followed by dehydration in ethanol and xylene. Finally, sections were cover-slipped and analyzed under a light microscope.

2.9 Ex vivo experiments

Pharmacological distribution studies were conducted on the ex vivo rabbit and eIBUB models. Spatial drug distribution was evaluated among and within organs based on the depth of tissue drug penetration and tissue drug concentration. Moreover, real-time measurements of tissue aerosol absorption and aerosol sedimentation were possible on eIBUB, including local toxicity. Finally, the application time of electrostatic precipitation was evaluated and modified on eIBUB.

2.9.1 Cadaveric experiments in rabbits

Study design

Intraabdominal doxorubicin distribution after ePIPAC was investigated in the ex vivo rabbit model. Two groups of three rabbits were assigned for ePIPAC as a test and PIPAC as a control. In ePIPAC, an electrostatic field was activated at the beginning of aerosolization and turned off 30min after it. In the control group, PIPAC following 30min exposure time was executed. At the end of the experiment, punch biopsies were taken from the abdominal wall, small intestine, colon, and stomach for qualitative and quantitative analyses.

Regulatory framework

According to the German Animal Welfare Low, no ethical approval has to be obtained for ex vivo experiments on animal organ wastes. Experiments on post-mortem rabbits were done after ophthalmological surgery and euthanization.

PIPAC and ePIPAC on a post-mortem Rabbit model

Six post-mortem rabbits 5-8kg after previous ophthalmological surgical experiments were subjects for PIPAC and ePIPAC studies.

PIPAC on ex vivo Rabbit model

In an exhaust hood, animals were placed in the supine position. Veress needle was injected under the left rib cage, and the 15mmHg pneumoperitoneum was insufflated. A trocar was inserted in the midline between the pubis and processus xiphoid. Capnopen® was inserted into the trocar. Doxorubicin and cisplatin were prepared for aerosolization as described in Chapter 2.6.3. Two Medtron® syringes with doxorubicin and cisplatin were consequently loaded to the injector Accutron HP-D® and connected with Capnopen® through a high-pressure line. Injection parameters were set up to injection flow 0.6ml/sec and injection volume

50ml for doxorubicin and 150ml for cisplatin. Drugs were consequently aerosolized following 30min exposure time. At the end of the experiment, punch biopsies were taken from the abdominal wall, small intestine, colon, and stomach for qualitative and quantitative analysis and frozen under -80ºC.

ePIPAC on ex vivo Rabbit model

In comparison with PIPAC, ePIPAC requires the generator of an electrostatic field with two electrodes. One electrode was inserted into the abdomen, and another one was stuck onto the advanced shaved back. The electrostatic field was activated at the beginning of the drug application and turned off 30min after it.

2.9.1.1 Depth of tissue penetration

Four biopsies from the abdominal wall, small intestine, colon, and stomach were analyzed per animal. Doxorubicin spontaneous fluorescence at 595nm was chosen for qualitative analysis. Biopsies

were mounted with an embedding medium on cryotome chucks and half-trimmed. Three 5-10µm cryosections per biopsy were transferred to a microscope slide, airdried, and coverslipped under a mounting medium. The quality of cryosections was examined under light microscopy, and the depth of doxorubicin penetration was measured in triplicate under fluorescence microscopy.

2.9.1.2 Drug tissue concentration

From each animal, three punch biopsies from the abdominal wall, small intestine, colon, and stomach were analyzed. Doxorubicin concentration per biopsy was quantified by high-performance liquid chromatography (HPLC, Waters Fluorescence Detector 2475, Waters Inc., Milford, MA, USA) in an external GLP-certified lab. For analyses, samples were dehydrated overnight, and then pellets were weighed and reconstituted in 1.5ml of distilled water, followed by homogenization at 50Hz for 2 hours and centrifugation at 11000rpm for 15min.

2.9.2 ePIPAC on eIBUB: optimization of application time

Study design

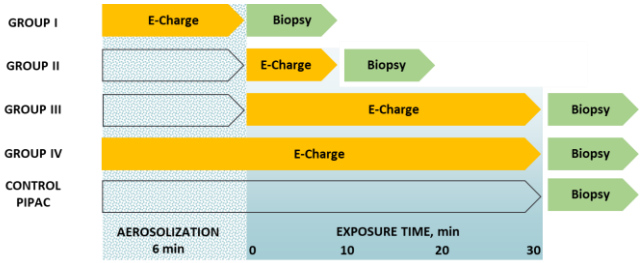

Figure 13. ePIPAC on eIBUB: optimization of application time.

Group I: e-charge 6min during PIPAC; group II: e-charge 10min after PIPAC; group III: e-charge 30min after PIPAC; group IV: e-charge 36min during and after PIPAC.

This study was conducted with an ex vivo eIBUB. Four groups were designed based on the activation time of an electrostatic field and one group as a control without the electrostatic field. Three bladders per group were assigned. The first group underwent PIPAC for 6min with simultaneous exposure to the electrostatic field. The second group

underwent PIPAC for 6min with the following activation of the electrostatic field for 10min. In the third group, PIPAC was conducted for 6min with subsequent activation of the electrostatic field for 30min. In the fourth group, the electrostatic field was activated at the beginning of PIPAC and turned off 30min after drug aerosolization. PIPAC with 30min exposure time was set as a control. At the end of each experiment, punch biopsies were taken for qualitative and quantitative analysis.

Hypothesis$_0$: there is no difference in tissue drug distribution among the four test groups and the control.

Regulatory framework

According to the German Animal Welfare Act, there is no need for regulatory approval for ex vivo experiments on organ wastes purchased from a slaughterhouse.

Experiments on eIBUB

Five bovine bladders cooled at 4º C were delivered from a slaughterhouse to our lab for each experiment. Bladders were rinsed with water, and surrounding tissue was dissected. The organ was inverted inside out, namely serosa inside, and mucosa outside. Three bladders without any damage and with nearly the same weight and length were selected for an experiment.

For the setup of the eIBUB model, a 20cm line was inserted at the bladder bottom and airtight with sutures. Trocar was inserted through the bladder neck with the following sutures. In the exhaust hood, the bladder was hung on a tripod placed on a scale. The airtight plastic cup was placed on a lab jack near the tripod and elevated to the level of the bladder bottom. The bladder was connected with a plastic cup through the 20cm line filled with water to prevent aerosol from escaping from the bladder. The

line from the CO_2 insufflator was split and connected to the plastic cup and trocar. The CO_2 insufflator was turned on, and a CO_2 pressure 15mmHg was achieved in both the plastic cup and the bladder. A spray nozzle Capnopen® was inserted in the bladder through the trocar. For generating an electrostatic field, an Ultravision® device (Alesi Surgical, Cardiff, UK) with two electrodes was implemented. The first electrode was placed at the top of the bladder, and the second electrode at the bottom. The activation of the generator is as per the experiment protocol (see above).

For drug aerosolization, 200ml Medtron® syringes filled with doxorubicin followed by cisplatin were loaded to injector Accutron HP-D® and connected via a high-pressure line with the spray nozzle Capnopen®. Injection parameters were set up to injection flow 0.6ml/sec, doxorubicin volume 50ml, and cisplatin volume 150ml.

The exhaust hood was turned on, and drug aerosolization was begun. The data from experiments were documented under the eIBUB protocol. At the end of the procedure, punch biopsies from the top x 8, middle x 8, and bottom x 8 were taken for qualitative and quantitative analyses and immediately frozen under -80º C. For qualitative analysis, biopsies were additionally labelled from the mucosa side to enable histological positioning. The rest of the organs were disposed of as biological waste.

2.9.2.1 Depth of tissue penetration

The depth of doxorubicin penetration was measured qualitatively and quantitatively. Liquid penetrating on the external surface of eIBUB was collected, and the thickness of the eIBUB wall was measured at the top, middle, and bottom. A liquid sample was investigated under a fluorescence microscope regarding spontaneous doxorubicin fluorescence at 595nm. The same liquid sample was sent to an

external GLP-certified lab for quantitative analysis of doxorubicin and cisplatin. Doxorubicin concentration was by high-performance liquid chromatography (HPLC, Waters Fluorescence Detector 2475, Waters Inc., Milford, MA, USA) and cisplatin by atomic absorption spectroscopy (AAS; ZEEnit P 650, Analytic Jena AG, Jena, Germany). If a liquid sample had positive spontaneous fluorescence or the presence of doxorubicin or cisplatin, the depth of drug penetration was considered equal to the eIBUB wall thickness.

2.9.2.2 Drug tissue concentration

Doxorubicin concentration was measured by HPLC. Nine biopsies per eIBUB were analyzed as follows 3 from the top, 3 from the middle, and 3 from the bottom. Preanalytical preparation was according to the protocol described in Chapter 2.9.1.2.

2.9.2.3 Real-time measurements of tissue uptake

eIBUB was placed on a scale that enables over-time measurements of tissue aerosol absorption. The difference in eIBUB weight before aerosolization and during/after it shows eIBUB drug absorption. The volume of liquid collected in the airtight cup reflects sedimented aerosol.

2.9.2.4 Real-time measurement of aerosol sedimentation

The volume of liquid collected in the airtight cup reflects sedimented aerosol and has been measured over time during and after aerosolization.

2.9.2.5 Homogeneity of spatial distribution

Spatial drug distribution was analyzed based on tissue drug concentration and depth of tissue penetration. Measurements were performed at three levels, namely the top, middle, and bottom of the bladders. The results were compared within and among the groups.

2.10 Statistical analysis

Descriptive and comparative statistics were processed by SPSS®.

2.10.1 Blinding

Tissue samples were blinded for origin and treatment and analyzed independently.

2.10.2 Descriptive statistics

Samples were grouped based on treatment mode and described by median and mean values, standard deviation, and confidence interval. The results of the qualitative and quantitative analysis are presented on dot-plot, boxplot, histograms, lines, and areas.

2.10.3 Comparative statistics

Obtained data were not normally distributed. Thus, one-way ANOVA for nonparametric data was applied. Statistical significance was achieved with a power of 80% and a standard error of 5%. The clinically relevant difference was considered by 25%.

3 Results

The differences between ePIPAC and PIPAC were observed in physical, in vitro, and ex vivo experiments. In the physical part, aerosol granulometry, sedimentation, and spray patterns were shown on blotting paper and in the real-time aerosol sedimentation model. In vitro, cell toxicity was investigated by viability assays and cell growth inhibition. Intrinsic and extrinsic ways of apoptosis were evaluated by IHC assays. Spatial doxorubicin distribution within abdominal organs was explored in the cadaveric rabbit model, and the application time of the electrostatic field was optimized in the eIBUB.

The results of this dissertation are partially published in [104].

3.1 Quality by design

The quality-by-design concept was proposed by M. Juran in 1992 [123] to improve the quality of

pharmaceutical products. Desired product qualities should be incorporated into product design and be carefully controlled at all development steps.

3.1.1 Quality target product profile (QTPP)

The Quality Target Product Profile (QTPP) describes the design criteria for the drug-device combination and should therefore form the basis for the development of the CQAs, CPPs, and control strategy.

Table 3. Quality Target Product Profile.

QTPP Elements	Target
Doxorubicin	
Dosage form	solution
Dosage design	Immediate release
Route of administration	Intraabdominal
Dosage/concentration strength	Ex vivo and in vivo 2.7mg; in vitro $2.49*10^{-5}$ mol/L
Pharmacokinetics	Immediate release enabling local T_{max} in 10min
Stability	>43d at RT
Syringe closure system	Syringe closure system qualified as suitable for this drug product

Solubility	In water 29mg/ml
Application temperature	18-25ºC
pH	4.9
Charge	positive
Viscosity	1cSt
Volume	50ml
Cisplatin	
Dosage form	solution
Dosage design	Immediate release
Route of administration	Intraabdominal
Dosage/concentration strength	Ex vivo and in vivo 13.5mg; in vitro $2.25*10^{-4}$ mol/L
Pharmacokinetics	Immediate release enabling local T_{max} in 10 min
Stability	>30d at RT
Syringe closure system	Vial closure system qualified as suitable for this drug product
Solubility	Water 1mg/ml
Application temperature	18-25ºC
pH	4.6
Charge	neutral
Viscosity	1cSt
Volume	150ml
Drug delivery system	
Injection flow	0.6-0.7ml/sec
Pressure in the system	10-20bar
Mean aerosol diameter	1-150µm
Drug delivery: physical factors	
Temperature intraabdominal	Ex vivo: 18-25ºC; In vitro: 37ºC
Temperature environmental	Ex vivo: 18-25ºC; In vitro: 37.0ºC

Humidity intraabdominal	Ex vivo: ≤95% In vitro: ≤95%
Humidy environmental	Ex vivo: 30-52%; In vitro: ≤95%
Electrostatic field	Ionwand current 1-10µA; Ionwand voltage 7000-10000V
Intraabdominal pressure	15mmHg
Abdomen expander	CO_2
Drug delivery: biological factors	
Age	Ex vivo (eIBUB): not defined; Ex vivo (Rabbits): 12 months; In vitro: 1 passage/3d
Biological gender	Ex vivo (eIBUB): not defined; Ex vivo (Rabbits): female; In vitro: not defined
General condition	Ex vivo (eIBUB): not defined; Ex vivo (Rabbites): normal; In vitro: initial viability >90%
Weight	Ex vivo (eIBUB): 90-200g; Ex vivo (Rabbits): 5000-7000g; In vitro: not defined
Lenght	Ex vivo (eIBUB): 10-40cm; Ex vivo (Rabbits): 40-60cm; In vitro: 170-270µm

BMI	Ex vivo (eIBUB): not defined; Ex vivo (Rabbits): 28-34kg/m^2; In vitro: not defined
Body surface	Ex vivo (eIBUB): 80-450cm^2; Ex vivo (Rabbits): 2400-2800cm^2; In vitro total: 30.72-57.6cm^2
Abdomen volume	Ex vivo (eIBUB): 0.1-5.0L; Ex vivo (Rabbits): 0.8-1.5L; In vitro: 0.019-0.054L/well
Previous local chemotherapy	No
Presence of fibrosis	No
Histology	Healthy
Tumor extension	No

Table 3 represents the Quality Target Product Profile for intraabdominal aerosol chemotherapy, consisting of drugs, drug delivery system, and physical and biological factors.

3.1.2 Critical quality attributes (CQAs)

Critical quality attributes are parameters that should be within a specific range to ensure desirable product quality.

Table 4. Critical quality attributes.

CQA Elements	Target
Tissue drug distribution	
Tissue concentration	Doxorubicin >5ng/ml Cisplatin >80ng/ml
Depth of penetration	>300µm
Homogeneity	Visceral=parietal peritoneum No vertical gradient No gradient within and among organs
Technological	
High-pressure injector	- High-pressure resistant lines over 20bar - Operating pressure limit 20bar - Injection flow 0.5-0.7 ml/sec
Spray nozzle	Optimal operating pressure 15-20bar
Electrostatic charge generator	- The minimal distance between the brush electrode and the target object 25mm - The brush electrode is soft - No alarm signal
Application	
Surgical time	Set up 15min Drug application ≤10min Procedure ending 10min

	Total surgery time under 165min [105]	
In-patient stay	0-1d	
Safety	safe for clinical and research staff patients' side effects CTCAE Grade 1-2	
Mean costs	6562 €/ 1 hospitalisation [105] < 100 €/ 1 experiement [106]	
Setting	Clinical: Operation room with laminar flow Protective clothes Certified surgeons Preclinical: Cytostatic approved bench Continuous room airflow Trained staff Protective clothes	
Applicability	Multiple applications >1	
Reproducibility	Established technology and standardized procedure	
Effectiveness		
Preclinical	Physical/ technological	- homogeneous aerosol - no aerosol aggregation overtime - MAD 1-30µm - homogeneous spray patterns
	in vitro	- Cell growth inhibition - Reducing cell metabolic activity - Apoptosis activation

	ex vivo	- See 'tissue drug distribution' - real time tissue aerosol absorption under 10min - real time aerosol sedimentation under 10min
	in vivo	- See 'tissue drug distribution' - Side effects CTCAE Grade 1-2 - Low tissue drug clearance - Delayed drug release
Clinical	Quality of life after surgery: Karnofsky Index ≥80% (considering 100% before) Survival: curative intention	
Histological	PRGS 1-3	

Table 4 shows the critical quality attributes required for product quality management and control.

3.1.3 Critical material attributes (CMAs)

Critical material attributes are a process or materials that influence critical quality attributes, thus modifying product quality.

Table 5. Critical material attributes.

CMA Elements	Target
Drugs	
Doxorubicin	Doxorubicin Doxo-Cell® 2mg/ml Cell Pharm® Ltd., Bad Vilbel, Germany
Cisplatin	Cisplatin-Teva® 0.5mg/ml, Teva Pharma AG Ltd., Ulm, Germany
NaCl 0.9%	University Clinic Pharmacy, Tuebingen, Germany
EU-certified technology for aerosol chemotherapy	
Injector	Accutron HP-Thera®, Medtron AG, Saarbrücken, Germany
Spray nozzle	Capnopen®, CapnoPharm Ltd., Tuebingen, Germany
High-pressure line	HS 224/150, Medtron AG, Saarbrücken, Germany
Electrostatic charge generator	Ultravision®, Alesi Surgical Ltd., Cardiff, UK
Preclinical setting	
Lab staff	Trained surgical residents and doctorates
Lab equipment	- Bench Thermo Scientific™ Maxisafe 2020 - Continuous room airflow - Permanently stable room climate under climate air conditioner - Validated pippets - QIAGEN tissue homogenizer - Thermo Scientific Savant SpeedVac vacuum concentrator

	- Validate analytical scales - Particle size analyser SprayTec etc.
Pharmacological measurements	Samples were prepared by lab staff and analysed in external GLP certified lab
Physical experiments	- Particle size analyzer SprayTec
In vitro experiments	- NHDF immortal cell culture line
Ex vivo experiments	- eIBUB model: bovine urinary bladders delivered immediately after explantation at 4°C - Rabbit model: rabbits euthonized after ophthalmological surgery were immediately underwent PIPAC and ePIPAC
In vivo experiments	Healthy animals anatomically, dimensionally and physiologically similar to human e.g. swine.
Clinical setting	
Trained surgical team	Certified PIPAC courses and trainings
Patient selection	Certified tumor boards
Certified technology	See ‘EU certified technology for aerosol chemotherapy‘
Unified histological regression score	e.g. PRGS

Table 5 illustrates the critical material attributes that have to be fulfilled to reach the desired product quality.

3.1.4 Risk assessments

The development of drug-device combinations requires a precise risk assessment focusing on the probability of problems occurring during the development process, their severity, and their influence on product quality. Risk assessment can be based on pilot studies, published work, previous research studies, and experts' opinions. In our study, developing a drug-device combination, we faced technological issues, safety questions, effectivity, applicability, and reproducibility risks. Our risk assessment was based on pilot studies, published work, and previous research experience.

Technology

Clinical-established PIPAC technology with EU-certified devices was applied based on more than

1500 PIPAC and ePIPAC procedures performed in our research unit. The following technological problems were considered:

Table 6. Risk assessment in technology.

Problem	Reason	Solution	Frequency
High-pressure injector			
Constant low battery charge	End of lifespan	Battery change	2 in 6 years
High-pressure alarm	High injection flow	Lower injection flow	Often by reused spray nozzle or the first test of a new spray nozzle
Spray nozzle			
Narrow spray angle	Low injection pressure	Higher injection flow	Often by the first test of new devices
Decreasing performance	Nozzle reuse	Nozzle change	After 3-5 applications
Increasing aerosol diameter	- Low pressure - Nozzle reuse	- Higher injecttion flow - Nozzle change	After 3-5 nozzle applications. Often by the first test of a new nozzle
Nozzle obstruction	High-viscosity	Nozzle change	Often by a test of viscose

	liquids, hydrogels		formulations over 5cSt
Electrostatic charge generator, Ultravision			
Proximity alarm	- Wet brush electrode - Distance between brush electrode and target under 25mm	- Dry brush electrode - Avoid direct contact of an aerosol stream with a brush electrode - Distance increase between brush electrode and target over 25mm	Often by a short distance between the brush electrode and the target

Table 6 represents the technological risks, including probability and possible solutions.

Applicability and reproducibility

The applicability and reproducibility were proven in physical experiments, in vitro and ex vivo, in over 1500 PIPAC and ePIPAC procedures. No critical

technical or set-up limitations were reported. All experiments were conducted as planned.

Safety

Air and surface contamination with cytotoxic drugs was investigated once a year. Operation with cytotoxics was strictly under a certified bench and continuous room airflow by an experienced and trained team in a protective cloth. Waste disposal was according to German regulations by internal clinical service.

Effectiveness

Risks in preclinical effectiveness were evaluated in physical, in vitro, and ex vivo experiments.

Preclinical

Table 7. Preclinical risk assessment.

Problem	Reason	Solution	Frequency
Physical experiments			
Laser background noise	Laser lens contamination	Lens cleaning	Rare, in a nozzle with a spray angle over 90°
In vitro			
Mechanical cell damage	Direct exposure to an aerosol stream	Increase distance between nozzle and cell culture plate	Not observed
Cytotoxic surface contamination	Small size of cell culture plates, not airtight except for flasks	Position of cell culture plate into an airtight plastic box	Not observed
No established electrostatic cell culture model for ePIPAC	No ePIPAC on cell culture was previously performed	- Establishment of an electrostatic cell culture model - If not possible,	The model was established

		no in vitro investigation in ePIPAC	
Ex vivo tissue drug distribution			
Tissue drug concentration under sensitivity threshold	- Low drug dosage - Low delivery rate of spray nozzle - Low analysis sensitivity - Drug damage during probe preparation - Organic debris	- If possible dosage increase - Improvement of aerosolising device - Probes analysis in GLP-certified lab - Avoid heating during probe preparation - Pilot studies - At least 3 probes per target	Rare in some probes
No fluorescence of doxorubicin	- Fluorescence filter does turn off or damaged - Low tissue drug concentration - Microscopy in a bright room or	- Positive controls by microscopy and tissue concentration analysis - Microscopy in the dark room, avoid probes exposure to light	Rare in some probes

	probes exposed to light	- At least 3 biopsies per target with 3 slides per biopsy and 3 measure-ments per slide	
Inhomoge-neous drug distribution	- Small number of tissue biopsies - Mecha-nical obstacles - Sedimen-ted liquid - Nozzle limitations	- Multiple samples, at least 3 from different regions - Capnoperi-toneum 15mmHg, laparoscopic video control - Evacuation of sedimented liquid over time, if possible - Nozzle improve-ment	Very often, caused mainly by nozzle limita-tions
Ex vivo eIBUB			
Mechanical tissue damage by explantation	Explanta-tion was performed in a slaughter-house	Precise organ selection	2 out of 10 urinary bladders

Tissue necrosis	Delay in delivery	- Delivery by internal clinic transport immediately after explantation at 4°C - Histologi-cal screening	Not observed
Aerosol leakage	Tissue damage, trocar or tubing leakage, open ureters	- CO_2 flow and volume check before aerosoli-zation - Ureters ligation - Additional purse string sutures around tubing and trocar	3 out of 10 urinary bladders
Cytotoxic environment-tal contamina-tion	Aerosol leakage	- CO_2 flow and volume check before aerosoliza-tion - Ureters ligation - Additional purse string sutures around tubing and trocar - All experiments in approved	Not observed

		bench for cytotoxic drugs	
Ex vivo rabbit model			
Tissue necrosis	Delay in delivery	- Delivery by internal clinic transport immediately after euthanasia at 4°C - Histologi-cal screening	Not observed
Aerosol leakage	Tissue damage, untied trocar	- CO_2 flow and volume check before aerosoliza-tion - Purse string sutures around the trocar	Not observed
Cytotoxic environment-tal contami-nation	Aerosol leakage	- CO_2 flow and volume check before aerosoliza-tion - Purse string sutures around the trocar - All experiments in approved bench for	Not observed

		cytotoxic drugs	

Table 7 shows risks in preclinical effectiveness and possible troubleshooting for physical, in vitro, and ex vivo experiments.

The risk assessment demonstrated no critical problems that might terminate the preclinical development process or deteriorate the product quality. For the occurring problems, multiple solutions and alternatives were proposed.

3.1.5 Design Space

Medicaments

Doxorubicin and cisplatin are the most often off-label used drugs in PIPAC and ePIPAC applied at RT and humidity.

Drug delivery system

The Capnopen® connected with a high-pressure injector was the drug delivery system implemented in this research. The Capnopen®, combined with a high-pressure injector, is EU-certified as a medical device for intraabdominal aerosol chemotherapy. Optimal aerosol generation was achieved as recommended by the manufacturer by an injection flow of 0.6-0.7ml/sec and pressure of 10-20 bar.

Drug delivery: physical factors

Ex vivo and lab stand physical experiments were conducted under 18-25ºC, predefined by the room air conditioning system. In vitro incubation was under 37.0ºC and during drug application at RT.

Humidity in ex vivo and laboratory stand experiments was 30-52%, controlled by an air conditioning system, and correlates with indoor

humidity. In vitro, incubation humidity was about 95%, during treatment at room temperature.

During ePIPAC, an electrostatic field was generated by the CE-certified Ultravision® system (Alesi Surgical, Cardiff, UK).

Capnoperitoneum 15mmHg was insufflated as recommended for standardized laparoscopy.

Drug delivery: biological factors

Lab stand physical experiments: not observed.

In vitro NHDF cell culture: age, gender, general condition, weight, and BMI were not defined. The length of one cell was 170-270µm. The total cell culture plate surface was 30.72-57.6cm^2, total culture plate volume 19.2-54ml, no previous chemotherapies, no signs of fibrosis, tumor free.

Ex vivo eIBUB: age, gender, general condition, and BMI were unknown. The length was 10-40cm and the weight was 90-200g. The surface was 80-

450cm^2, the volume range 0.1-5.0L, no previous chemotherapies, no signs of fibrosis, tumor free.

Ex vivo rabbit model: age 12 months, gender female, good general condition, BMI 28-34kg/m^2. The length was 40-60cm and the weight was 5000-7000g. The surface was approximately 2400-2800cm^2, volume range not applied, no previous chemotherapies, no signs of fibrosis, tumor free.

3.2 Physical experiments

Overtime aerosol sedimentation was measured in PIPAC and ePIPAC by laser diffraction. Spray patterns after both procedures were observed on 2D and 3D blotting paper.

3.2.1 Granulometry

PIPAC

MAD and laser transmission were measured during aerosol generation and 10min exposure time. Enlargement of aerosol particles was observed in all

three measurements during the exposure time. The presence of floating aerosol was additionally confirmed by transmission.

Table 8. Overtime granulometry during PIPAC.

Measurement	Plateau (µm)	Whole-time analysis (µm)		
	Dx50	Dx10	Dx50	Dx90
1	21.49	27.05	166.80	495.30
2	25.46	20.76	77.47	135.90
3	30.14	24.68	54.33	357.60
Mean (µm)	25.69	24.16	99.53	329.6

The results of granulometry during PIPAC are presented in Table 8. All measurements were in triplicate following the calculation of the mean value. The column "Plateau (µm)" gives an overview of MAD during aerosolization, with a mean value of 25.69µm. The whole-time analysis demonstrates particle size distribution at Dx10, 50, and 90 during the total experiment. The mean of “Whole-time analysis” Dx50 was 3.9 times higher

than the mean of "plateau", showing over time particle size growth after aerosolization.

Table 9. Overtime transmission after PIPAC.

Measurement	Application (sec)		Exposure (sec)
	86		≈ 506
	Mean transmission (%) regarding aerosolization		
	before	during	after
1	94.7	31.2	90.5
2	92.7	29.1	91.1
3	97.5	30.1	92.9
Mean (%)	94.97	30.13	91.5

The relative transmission before, during, and after PIPAC is presented in Table 9. The transmission during aerosolization was about three times lower than the initial one and did not wholly recover after 514sec.

ePIPAC: setup 1.

In setup 1, electrostatic precipitation was after aerosolization until the end of the experiment. MAD was stable during the measurement. Exposure time

was considerably shorter than in PIPAC due to complete aerosol precipitation.

Table 10. Overtime granulometry after ePIPAC. Setup 1.

Measurement	Plateau (μm)	Whole-time analysis (μm)		
	Dx50	Dx10	Dx50	Dx90
1	26.29	24.82	27.57	153.40
2	26.71	26.06	24.49	434.20
3	26.68	25.67	28.33	273.60
Mean (μm)	26.56	25.52	26.79	287.07

The data in Table 10 demonstrate the mean aerodynamic diameter of aerosol during ePIPAC. The column "Plateau (μm)" explains MAD during aerosolization and "Whole-time analysis (μm)" - during the whole experiment. At the end of each column, mean values are presented. The difference in mean MAD at Dx50 between the whole-time and plateau was 0.23μm, which confirms no substantial growth during the exposure time.

Table 11. Overtime transmission after ePIPAC. Setup 1.

Measurement	Application (sec)		Mean exposure (sec)
	86		≈ 16
	Mean transmission (%) regarding aerosolization		
	before	during	after
1	96.0	33.8	91.8
2	96.1	33.5	91.5
3	93.1	32.8	92.2
Mean (%)	95.07	33.37	91.83

Transmission before, during, and after aerosolization is shown in Table 11. During aerosol generation, the mean transmission was 2.85 times lower than before, and at the end of exposure time, 3.24% lower than the initial level. The time of aerosolization was 86sec and exposure – ≈16sec.

ePIPAC: setup 2.

Setup 2 with electrostatic precipitation during and after aerosolization demonstrated the same features as 1. No substantial MAD increase was seen. Given

space was cleared from aerosol within seconds after aerosolization.

Table 12. Overtime granulometry after ePIPAC. Setup 2.

Measurement	Plateau (µm)	Whole-time analysis (µm)		
	MAD	Dx10	Dx50	Dx90
1	26.41	24.47	27.26	145.00
2	26.37	25.40	27.66	145.20
3	26.64	25.48	30.16	286.50
Mean (µm)	26.47	25.12	28.36	192.23

Table 12 gives an overview of the mean aerodynamic distribution of aerosol particles during ePIPAC. The column "Plateau (µm)" presents MAD during aerosol generation and "Whole-time analysis (µm)" – during the whole experiment. The mean MAD at Dx50 after whole-time is 1.89µm higher than in the plateau showing no substantial difference or particle growth.

Table 13. Overtime transmission after ePIPAC. Setup 2.

	Application (sec)		Mean exposure (sec)
Measurement	86		23
	Mean transmission (%) regarding aerosolization		
	before	during	after
1	97.8	43.7	99.3
2	97.4	36.7	88.5
3	98.0	34.0	96.1
Mean (%)	97.73	38.13	94.63

Overtime transmission before, during, and after aerosolization is presented in Table 13. During aerosol generation, the mean transmission was 2.56 times lower than before, and at the end of the experiment, 3.1% lower than at the beginning.

3.2.2 Real-time aerosol sedimentation

MAD and laser transmission were depicted as a chart by Spraytec® software. The enlargement of aerosol particles was shown in PIPAC. ePIPAC demonstrated stable MAD and considerably shorter exposure time than PIPAC.

PIPAC

Granulometry was conducted during PIPAC with distilled water. The time of observation was 10min after aerosolization.

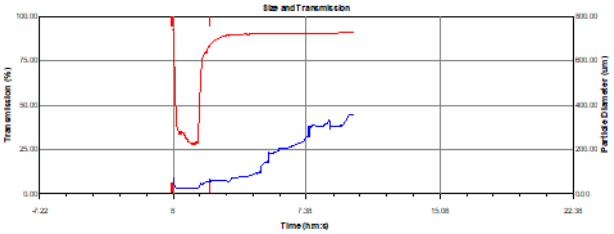

Figure 14. Measurement 1. Real-time median aerodynamic diameter and transmission during PIPAC.

Real-time median aerodynamic diameter (blue line) and transmission (red line). Aerosol was generated by Capnopen® from 60ml distilled water.

Figure 14 gives an overview of one of three measurements of MAD and transmission during PIPAC. The MAD line is going rapidly down and stabilizing at 30.14µm for 68sec. The stepwise growth over the next 546sec led the MAD line to cross the 350µm threshold by the end of 10min. The

transmission line hit a low under 35% for 68sec, then rapidly picked up over 85% by 150sec and slowly rose over the next 463sec. Measurements 2 and 3 are presented in the Appendix Physical experiments, PIPAC, Figures 40 and 41.

ePIPAC: setup 1.

Setup 1 indicates electrostatic field activation after aerosolization until the end of the experiment. The measurement was completed if no signal from the laser was obtained (bold red line on a chart) or 10min after aerosolization.

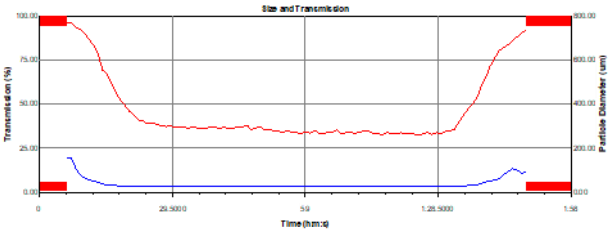

Figure 15. Measurement 1. Real-time median aerodynamic diameter and transmission during ePIPAC. Setup 1

Real-time median aerodynamic diameter (blue line) and transmission (red line). Setup 1: e-charge applied after aerosolization. Aerosol was generated by Capnopen® from 60ml distilled water.

Figure 15 depicts the MAD line decreasing in the first 12sec and turning into a plateau at 26.29µm for 78sec. In the last 13sec, the line goes up over 100µm. The transmission follows MAD by rapidly dropping by 21sec below 35%, slightly decreasing for 65sec, and quickly recovering the final 17sec over 91.8%. The measurement was stopped by SprayTec® after 103sec due to complete clearance of measurement space. Measurements 2 and 3 can

be found in Appendix: Physical experiments, ePIPAC: setup 1, Figures 42 and 43.

ePIPAC: setup 2.

The electrostatic field was activated before aerosolization and turned off at the end of the experiment.

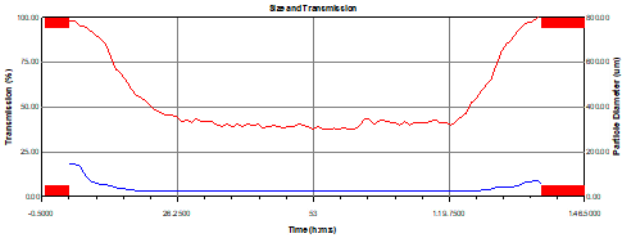

Figure 16. Measurement 1. Real-time median aerodynamic diameter and transmission during ePIPAC. Setup 2.

Real-time median aerodynamic diameter (blue line) and transmission (red line). Setup 2: e-charge for the whole experiment. Aerosol was generated by Capnopen® from 60ml distilled water.

Measurement one presents the MAD line gradually decreasing for 12sec, turning into a plateau at 26.41µm for 70sec, and slowly recovering over

50µm for 11sec. The transmission line follows MAD patterns by steeply decreasing for 19sec, stagnating under 50% for 57sec, and rising above 99% in 17sec. The experiment was for 93sec. Measurements 2 and 3 are shown in Appendix, Physical experiments, ePIPAC setup 2, Figures 44 and 45.

3.2.3 Spray patterns: 2D and 3D

Blue ink was aerosolized on flat (2D) and conical folded (3D) blotting paper during PIPAC and ePIPAC. The blue-stained surface was qualitatively and quantitatively analyzed by ImageJ®.

2D Model

ePIPAC on 2D demonstrated a more homogenous ink distribution among all three zones as PIPAC. However, PIPAC delivered a higher volume of ink to the furthest point from the nozzle, namely to the third zone.

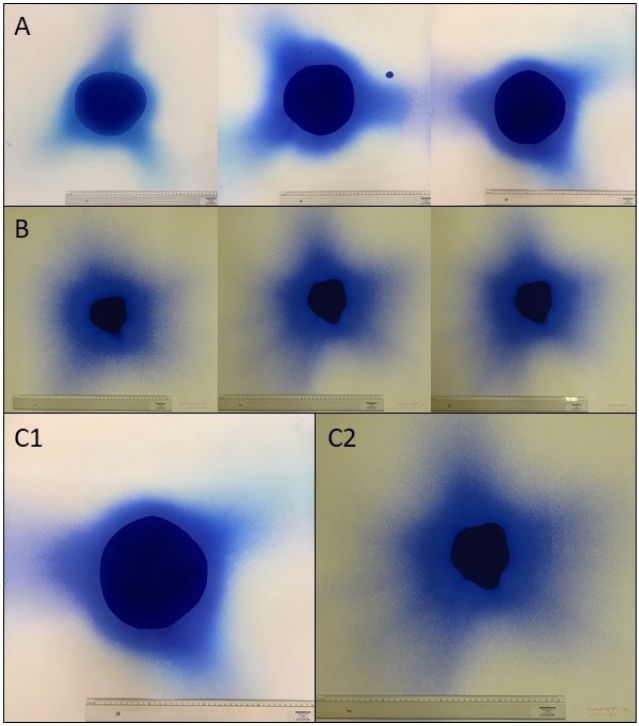

Figure 17. 2D (planar) blotting paper: spray patterns after ePIPAC and PIPAC.

ePIPAC panel A, C1 vs. PIPAC panel B, C2.

Figure 17 shows differences in spatial ink distribution on 2D (planar) blotting paper after ePIPAC and PIPAC. In both procedures, distribution was inhomogeneous.

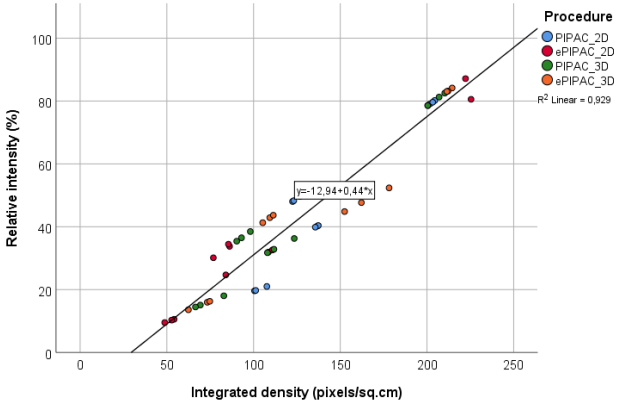

Figure 18. Correlation between relative intensity and integrated density.

The linear correlation between relative intensity and integrated density with r^2=0.93 was revealed and demonstrated in Figure 18. Increasing the relative intensity by 10% causes integrated density to rise by 22.73 units, which can be applied to predict one parameter by knowing another in spatial distribution studies.

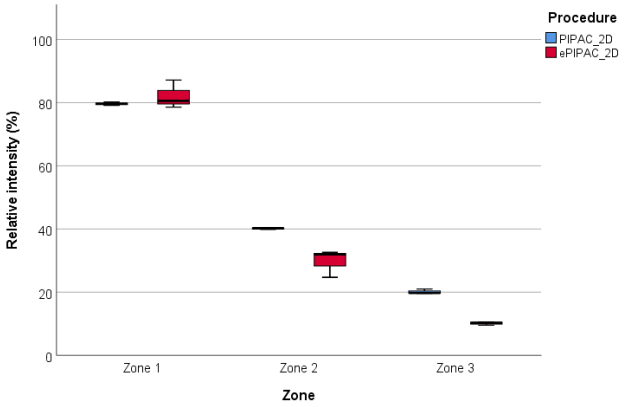

Figure 19. 2D (planar) blotting paper model. Relative intensity after ePIPAC vs. PIPAC among zones.

The mean relative intensity for PIPAC and ePIPAC in zone one was 79.65±0.51% and 82.09±4.49%, in zone two 40.16±0.26% and 29.74±4.40%, and in zone three 20.12±0.77% and 10.12±0.55%. Both procedures demonstrated a significant decrease in relative intensity from zone one to three ($p<0.005$). PIPAC had higher intensity in zone two and three than ePIPAC. The difference between ePIPAC and PIPAC in zone one was not significant ($p>0.05$) but in zone two and three ($p<0.05$).

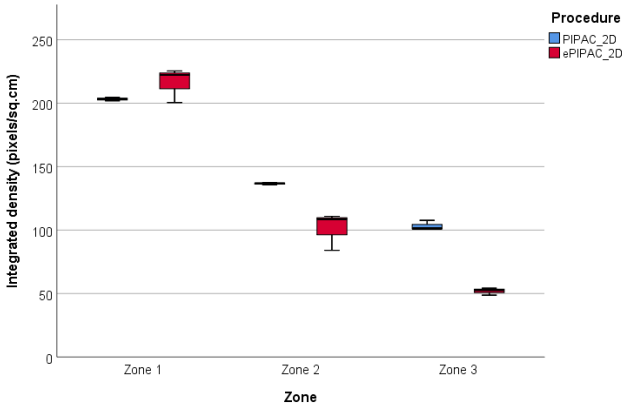

Figure 20. 2D (planar) blotting paper model. Integrated density after ePIPAC vs. PIPAC.

Integrated density after PIPAC and ePIPAC in zone one was 203.18±1.31pixels/cm^2 and 216.04±13.54pixels/cm^2, in zone two 136.56±.87pixels/cm^2 and 101.15±14.91pixels/cm^2 and in zone three 103.15±3.91pixels/cm^2 and 51.90±2.81pixels/cm^2. Integrated density significantly declined from zone one to three in both procedures ($p<0.005$). The numbers were significantly higher in PIPAC vs. ePIPAC in zone two and three ($p<0.05$).

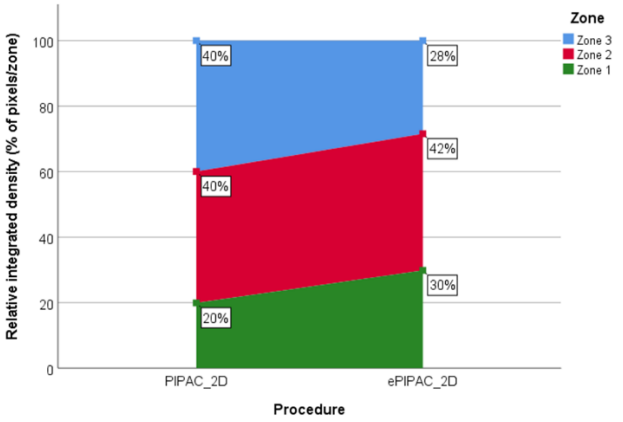

Figure 21. Ink distribution on the 2D (planar) model after PIPAC vs ePIPAC among zones.

Relative integrated density in Figure 21 shows ink distribution after PIPAC vs ePIPAC. In PIPAC, 20% of aerosolized volume reached zone one, 40% zone two, and 40% zone three. In ePIPAC, 20% reached zone one, 42% zone two, and 28% zone three. The proportion between zones for PIPAC 2:4:4 and ePIPAC 3:4:3. In PIPAC, differences between zone one and two, one and three were significant ($p<0.001$), and in ePIPAC, between one and two and

two and three. The difference in PIPAC vs ePIPAC was significant in zones one and three ($p<0.005$).

3D model

On the 3D model, PIPAC showed more homogenous ink distribution than ePIPAC and delivered the highest volume of ink to the third zone.

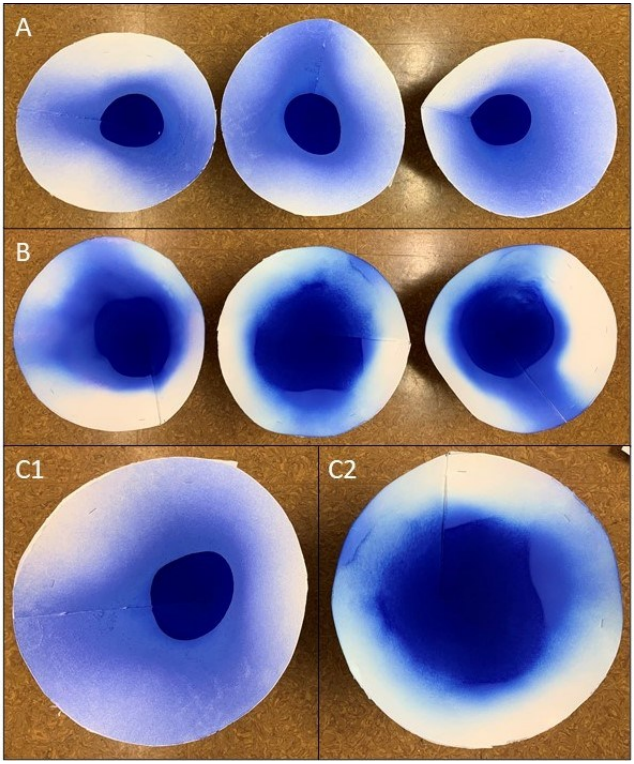

Figure 22. 3D (volumetric) blotting paper: spray patterns after PIPAC and ePIPAC.

Panel A and C1 – PIPAC; B and C2 – ePIPAC.

Spray patterns on 3D blotting paper after PIPAC and ePIPAC are presented in Figure 22. ePIPAC displays more intense and broader coloration in the

central part than PIPAC. However, ink distribution was inhomogeneous after both procedures.

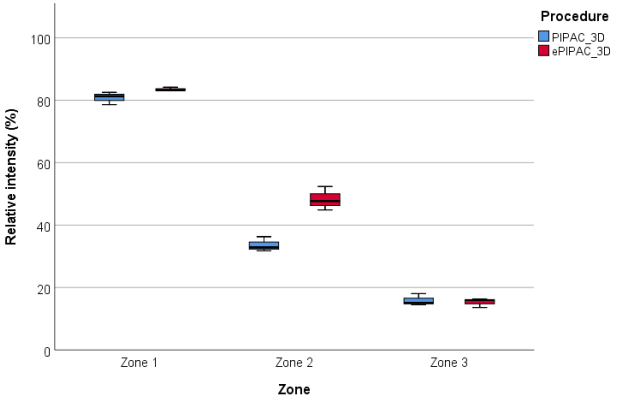

Figure 23. 3D (volumetric) blotting paper model. Relative intensity after PIPAC vs ePIPAC among zones.

Relative intensity after PIPAC and ePIPAC in zone one was 80.79±2.02% and 83.46±0.61%, in zone two 33.62±2.36% and 48.30±3.80%, and in zone three 15.87±2.36% and 15.28±1.47%. Both procedures showed significant intensity reduction from zone one to three ($p<0.001$). ePIPAC had

significantly higher intensity in zone two over PIPAC (p=0.005).

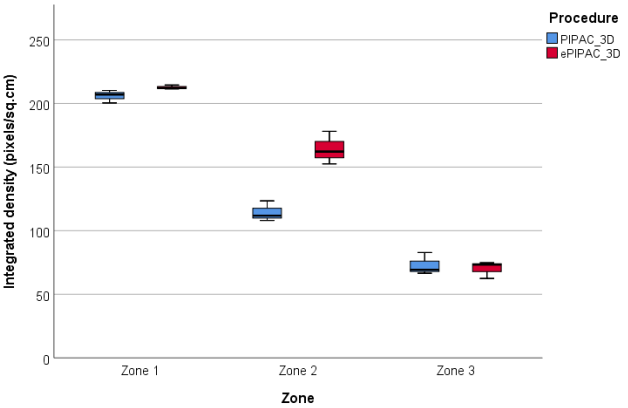

Figure 24. 3D (volumetric) blotting paper model. Integrated density PIPAC vs ePIPAC.

Integrated density after PIPAC and ePIPAC in zone one was 205.88±5.01pixels/cm^2 and 212.69±1.60pixels/cm^2, in zone two 114.41±8.05pixels/cm^2 and 164.27±12.96pixels/cm^2, in zone three 72.88±8.73pixels/cm^2 and 70.15±6.75pixels/cm^2. A significant decrease from zone one to three was observed in both procedures (p<0.005). ePIPAC had

a significantly higher integrated density in zone two over PIPAC (p=0.005).

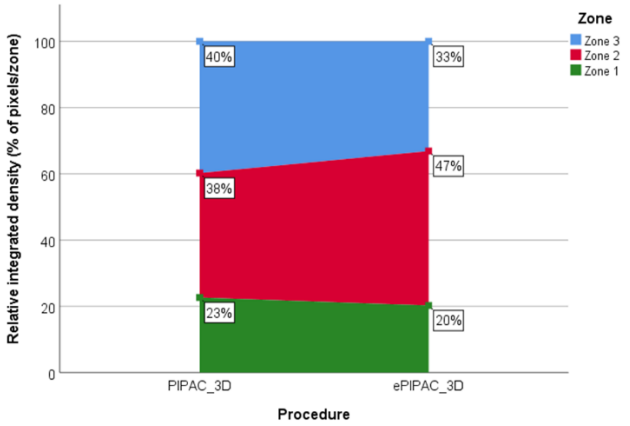

Figure 25. 3D (volumetric) blotting paper model. Total relative integrated density after PIPAC vs ePIPAC.

Figure 25 shows spatial ink distribution on 3D blotting paper based on total relative integrated density. The distribution of ink between zones after PIPAC and ePIPAC was in zone one 22.64±1.42pixels/cm^2 and 20.23±1.31pixels/cm^2, zone two 37.58±0.39pixels/cm^2 and 46.63±1.07pixels/cm^2 and zone three

39.78±1.63pixels/cm^2 and 33.15±1.27pixels/cm^2. The proportion among zones in PIPAC and ePIPAC was 2:4:4 and 2:5:3. The difference between zone one and two, one and three, was significant after PIPAC ($p<0.001$), and in ePIPAC significant difference was among all zones ($p<0.001$). ePIPAC had a significantly higher distribution in zone two vs PIPAC ($p<0.005$) but lower in zone three ($p<0.001$).

3.2.4 ePIPAC physical differences over PIPAC

Over time granulometry demonstrated more than 20 times longer aerosol floating after PIPAC vs ePIPAC. Electrostatic charge applied during and after aerosolization showed no considerable difference in aerosol floating time 1:1.1. The MAD constantly increased in PIPAC from 25.69µm to 99.53µm or for 4 times, and in ePIPAC no significant growth was observed in both groups, 26.5 µm to 27.68µm or 1:1.04.

In the blotting paper, distribution patterns after PIPAC and ePIPAC were analyzed. The relative integrated density and relative intensity on 2D and 3D models decreased significantly from zone one to three in both groups. This data shows the highest distribution to be in zone one and the lowest in zone three. The integrated density normalized to the total surface conveys PIPAC to deliver ≈10% more volume to zone three in the 2D and 3D models compared to ePIPAC. In the 3D model, ePIPAC delivers ≈10% more volume to zone two than PIPAC, and in the 2D model, ≈10% more to the first zone.

To sum up, PIPAC delivers higher volume to the furthest point from the spray nozzle and has a more homogeneous distribution than ePIPAC between zone two and three. At the same time, ePIPAC prevents the enlargement of aerosol particles and reduces the time of aerosol floating utilizing electrostatic precipitation.

3.3 In vitro experiments

Cell toxicity after PIPAC vs ePIPAC was investigated in viability assays and growth inhibition study. Intrinsic and extrinsic apoptosis was qualitatively and quantitatively analyzed by IHC.

3.3.1 Cell Viability Assays

Cell viability in 0h, 24h and 48h after PIPAC and ePIPAC was quantified by microscopy assay, FACS and MTT. A significant difference between both test groups was observed in 0h after the treatment, but not after 24h and 48h.

3.3.2 Annexin V/PI microscopy assays

Apoptosis was evaluated with microscopy assays immediately after the treatment. ePIPAC demonstrated a significantly higher number of apoptotic cells than PIPAC. Nonetheless, controls showed the opposite.

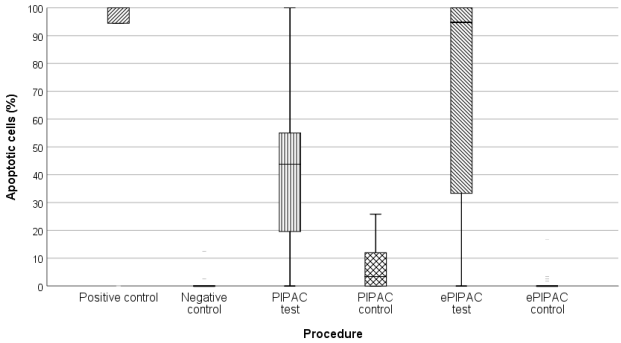

Figure 26. Annexin V/PI assay immediately after treatment.

The relative number of apoptotic cells immediately after PIPAC and ePIPAC is presented in Figure 26. After ePIPAC 68.48±39.16% of cells turned apoptotic and after PIPAC 43.03±27.93% ($p<0.05$). The controls demonstrated 0.93±3.32% of apoptotic cells after ePIPAC and 7.35±2.76% after PIPAC ($p=0.001$). The difference between the test and control/negative control was significant in both groups ($p<0.001$).

In the positive control, 90.85±39.06% of the cells were apoptotic, and in the negative control,

0.72±2.76%. The significant difference was between the PIPAC test and the positive control ($p<0.001$) but not between the ePIPAC test and the positive control ($p>0.05$). The difference between negative control and PIPAC control was significant ($p<0.005$), but between ePIPAC control and negative control, not ($p>0.05$). Positive control was significantly higher over PIPAC and ePIPAC controls ($p<0.001$).

3.3.3 Annexin V/PI FACS

Apoptotic cells were counted by FACS 24h after the treatment. No significant difference was between PIPAC and ePIPAC.

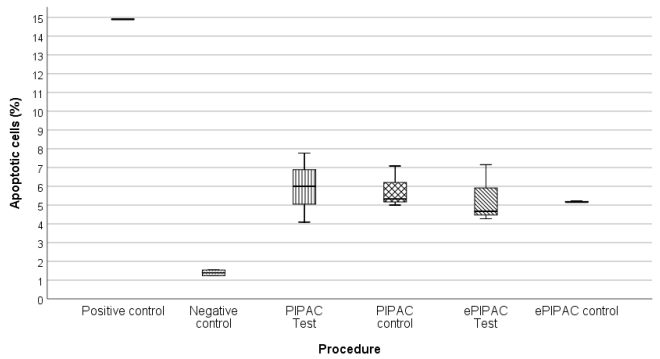

Figure 27. FACS with Annexin V/PI 24h after treatment.

Figure 27 represents the relative number of apoptotic cells 24h after the treatment analyzed by FACS. In the PIPAC test, 5.95±1.84% of cells were apoptotic, and in the ePIPAC test 5.36±1.56% ($p>0.5$). In the PIPAC control, 5.80±1.12%, and ePIPAC control, 5.18±0.04% ($p>0.05$). The positive control had 14.9% of apoptosis and the negative control 1.39±0.21%. The difference between the test and control was not significant ($p>0.5$) but between the test and negative control ($p<0.05$). There was no significant difference between the positive control

and PIPAC test ($p=0.052$) but between the positive control and ePIPAC test ($p<0.05$). The difference between the positive control and group controls was significant ($p<0.05$). Negative control and control groups demonstrated a significant difference ($p<0.05$).

3.3.4 MTT-Assays

Cell viability 48h after the treatment was measured by MTT assay. The PIPAC and ePIPAC test groups showed no significant difference. The ePIPAC control had significantly lower viability than PIPAC.

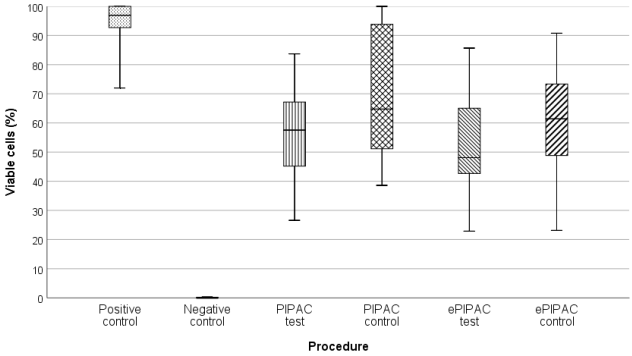

Figure 28. MTT-Assay. Cell viability 48h after treatment.

Cell viability 48h after PIPAC vs ePIPAC in control and test groups.

MTT-assay 48h after the treatment showed 56.51±14.98% viability after PIPAC and 51.82±13.83% after ePIPAC ($p=0.053$). In the PIPAC control, there were 75.60±29.93% viable cells, and in the ePIPAC control 61.15±16.87% ($p<0.001$). General control had 100% viability and a negative one of 0.003%. The difference between the test and control was significant ($p<0.001$). Positive control had significantly higher viability than the test and control groups ($p<0.001$).

3.3.5 Cell Growth Inhibition Study

Cell count was on each third day after PIPAC and ePIPAC at six-time points. On day three, around 60% of cells were dead in both test groups. Complete growth inhibition was on day 9. In controls, no significant difference was from day 1-9, but from 12-15. In ePIPAC control, the cell number was significantly lower on day 15 vs 3, but the opposite in PIPAC.

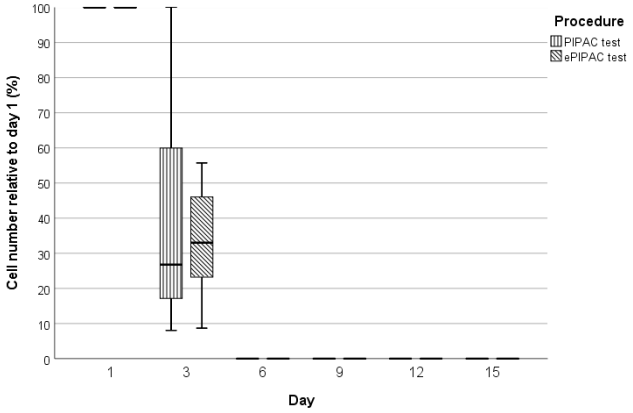

Figure 29. Cell growth inhibition after PIPAC vs ePIPAC. Test groups.

Figure 29 represents the relative median cell number over time after PIPAC and ePIPAC. On the first day, the treatment was conducted with a relative mean cell number of 100% in both groups. On the third day, the relative cell number was 37.5±29.42% in PIPAC, and in ePIPAC, 40.88±28.90% ($p>0.5$). On the sixth day in PIPAC was 7.2±21.14% cells, and in ePIPAC, 3.68±8.93%. On day nine, in PIPAC was 0.66±1.93% cells, and in ePIPAC, 0%. In the next measurements, complete cell growth inhibition was in both groups. The difference in the cell number in PIPAC between the first and third day was significant ($p<0.05$), but in ePIPAC, not ($p>0.05$). On the third day, the number of cells in the PIPAC test was significantly lower than in the control ($p<0.005$), but not in ePIPAC ($p>0.05$).

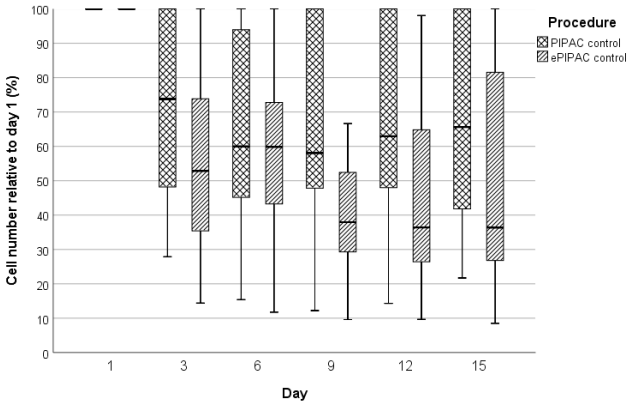

Figure 30. Cell growth inhibition after PIPAC vs ePIPAC. Control groups.

The median relative cell number in the control groups is presented in Figure 30. On day one, the mean relative cell number was 100% in PIPAC and ePIPAC. Treatment with 0.9% NaCl was performed. On day three, in PIPAC, cell number was 78.46±39.48%, and in ePIPAC 62.60±45.00% ($p>0.05$). On day six, in the PIPAC group, there was 68.80±33.09% of cells, and in ePIPAC 70.71±55.69% ($p>0.5$). On day nine, PIPAC 72.08±40.48% of cells and ePIPAC 42.47±22.47%

($p<0.05$). Day 12, PIPAC 75.31±42.30% and ePIPAC 45.55±26.06% ($p<0.05$). Day 15, PIPAC 99.29±67.63% and ePIPAC 47.28±32.01 ($p<0.05$). There was a significant difference in the cell number between days 1 and 3 in PIPAC ($p<0.05$) and ePIPAC ($p<0.005$), but not between days 3 and 15 ($p>0.05$).

3.3.6 Cleaved caspase-3

Cleaved caspase-3 predisposes intrinsic and extrinsic apoptosis. Qualitative and quantitative analysis was done by IHC.

3.3.7 Cleaved Caspase-3: qualitative Apoptosis Analysis

Histologically, the quality of samples after ePIPAC and PIPAC on eIBUB was analysed. In total, 560 pictures were taken. Serosa, muscles and mucosa were investigated based on cell staining and intracellular gaps.

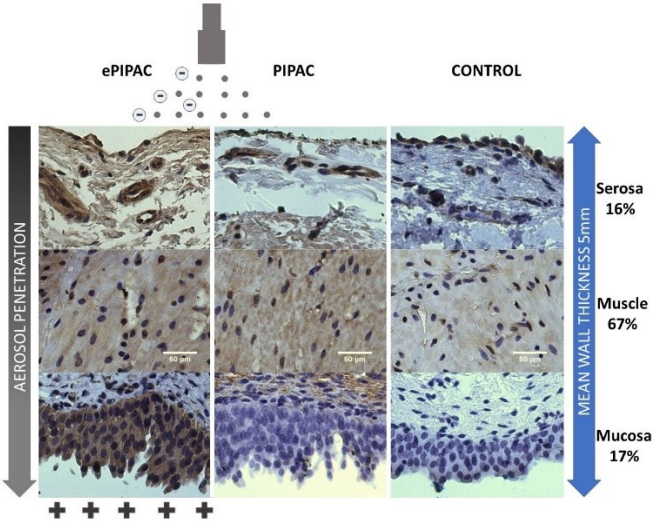

Figure 31. Cleaved Caspase-3 was investigated by IHC after ePIPAC and PIPAC on eIBUB.

PIPAC and ePIPAC groups were compared with untreated control. Serosa, muscle, and mucosa were analyzed on the presence of staining and gaps between fibres. The grey arrow indicates the direction of aerosolization and further drug penetration. The blue arrow shows the mean thickness of the bladder wall consisting of serosa in 16%, muscles in 67%, and mucosa in 17%. In ePIPAC, aerosol was negatively charged and tissue positively. In PIPAC, no charge was applied.

Cleaved Caspase-3 positive cells were found in all three groups except for technical controls. More

intensive staining of mucosa was in ePIPAC. Massive serosa cleavage was after ePIPAC and PIPAC.

3.3.8 Cleaved Caspase-3: quantitative Apoptosis Analysis

The number of cleaved caspase-3 positive nuclei was counted after ePIPAC and PIPAC on eIBUB. In control, no treatment was performed. Tissue biopsies were taken after the experiment, embedded into a paraffin block, cut, and stained with specific antibodies.

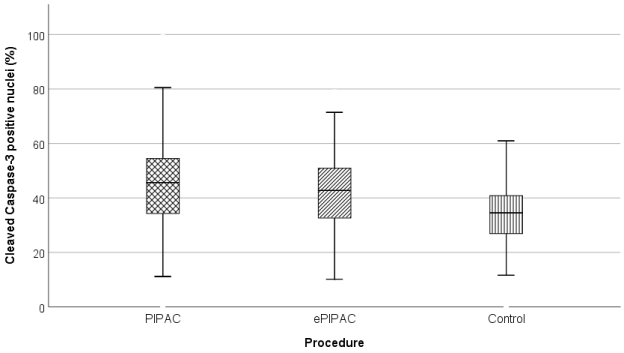

Figure 32. The relative number of cleaved caspase-3 positive nuclei after ePIPAC, PIPAC, and control. Biopsies from eIBUB.

In ePIPAC, the number of cleaved caspase-3 positive nuclei was 41.92±12.49%, in PIPAC 43.19±19.77%, and in control 31.54±13.76%. The difference between ePIPAC and PIPAC was not significant ($p>0.05$), but vs. control ($p<0.001$).

3.3.9 In vitro ePIPAC vs PIPAC: An Overview

ePIPAC and PIPAC significantly reduced cell viability compared to controls. The number of apoptotic cells was higher immediately after ePIPAC vs PIPAC ($p<0.05$), but not after 24h

(p>0.5). Cell toxicity assay showed no difference between both groups after 48h (p>0.05). Around 60% of cells turned to debris on day 3 after PIPAC and ePIPAC (p>0.05). On day 6, less than 10% of cells were viable in both groups and on day 9, complete growth inhibition was observed. Controls demonstrated continued cell growth. Apoptosis through intrinsic and extrinsic ways was activated in both groups. The number of cleaved caspase-3 positive cells was not significantly different after ePIPAC vs PIPAC (p>0.05).

3.4 Ex vivo experiments

Pharmacological analyses of ePIPAC vs PIPAC were performed in cadaveric rabbit and eIBUB models. Doxorubicin distribution within abdominal organs was explored in rabbits, and the application time of the electrostatic field was optimized in eIBUB.

3.4.1 Cadaveric experiments in rabbits

Cadaveric rabbits were undergone ePIPAC and PIPAC. Punch biopsies were taken from the small intestine, colon, stomach, and abdominal wall. The depth of doxorubicin penetration and tissue concentration were analyzed in the samples.

3.4.1.1 Depth of tissue penetration

Overall, doxorubicin tissue penetration was significantly higher in PIPAC vs ePIPAC, but the standard deviation was about three times lower in ePIPAC.

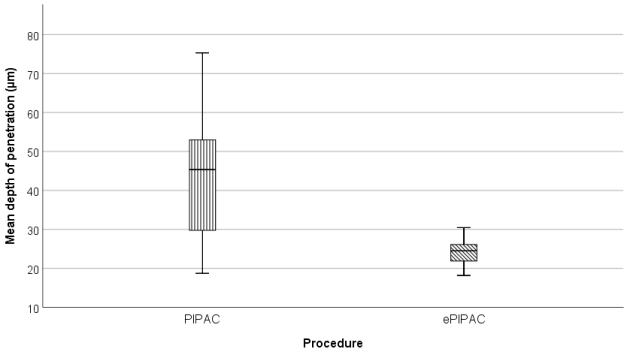

Figure 33. PIPAC vs ePIPAC in the ex vivo Rabbit model. The median depth of doxorubicin penetration is expressed in µm.

The mean depth of doxorubicin penetration after PIPAC was 43.05±13.88µm and after ePIPAC 24.93±4.28µm ($p<0.001$).

Between single organs, PIPAC showed a significantly higher depth of doxorubicin penetration over ePIPAC, but the standard deviation was smaller after ePIPAC in most of the cases. Within the group, ePIPAC had higher homogeneity vs PIPAC.

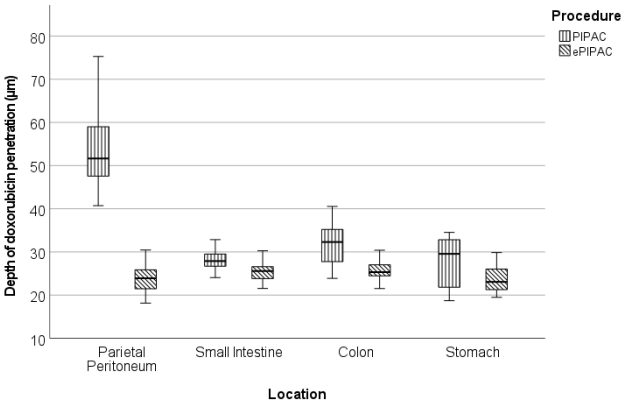

Figure 34. The median depth of doxorubicin penetration after PIPAC vs ePIPAC in ex vivo rabbit among organs.

Overall, the mean depth of doxorubicin penetration in the parietal peritoneum was 53.42±7.92µm after PIPAC and 24.88±5.15µm after ePIPAC ($p<0.001$). Penetration in the wall of the small intestine was 27.99±2.26µm and 25.41±2.41µm after PIPAC and ePIPAC ($p<0.001$), in the colon penetration after PIPAC was 31.61±5.00µm and ePIPAC 25.83±2.28µm ($p<0.001$), as well as 27.66±5.65µm after PIPAC and 23.76±3.08µm after ePIPAC ($p<0.005$) in the stomach. The difference of

penetration after PIPAC between the parietal peritoneum and small intestine, parietal peritoneum and colon, parietal peritoneum and stomach, and finally small intestine and colon ($p<0.001$), as well as colon and stomach, was statistically significant ($p<0.05$). No significant difference was measured after PIPAC between the small intestine and stomach ($p>0.5$). There was no significant difference after ePIPAC between the parietal peritoneum and small intestine, parietal peritoneum and colon, parietal peritoneum and stomach, small intestine and colon ($p>0.05$), but between small intestine and stomach as well as colon and stomach ($p<0.05$).

3.4.1.2 Drug tissue concentration

Doxorubicin concentration was measured in tissue biopsies by HPLC. Although the mean overall doxorubicin concentration was higher in ePIPAC vs PIPAC, significance was not reached. The standard

deviation was about 6 times lower after PIPAC vs ePIPAC.

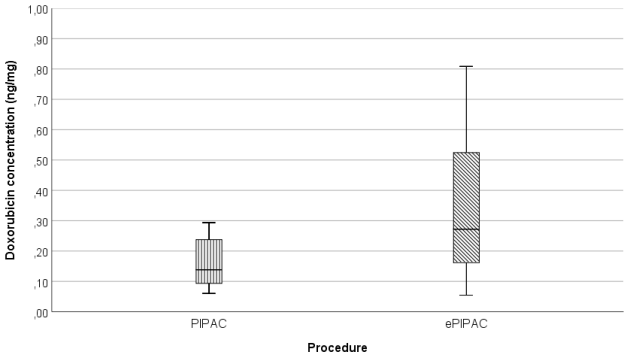

Figure 35. Median total doxorubicin concentration after PIPAC vs ePIPAC in ng/mg.

The overall mean doxorubicin concentration after PIPAC was 0.15±0.09ng/mg and ePIPAC 0.48±0.57ng/mg ($p>0.05$).

Spatial drug distribution showed a significantly higher doxorubicin concentration in the stomach after ePIPAC vs PIPAC. However, the standard deviation was around 9 times lower in PIPAC. In

spite of the high range, doxorubicin distribution was more homogeneous in ePIPAC vs PIPAC.

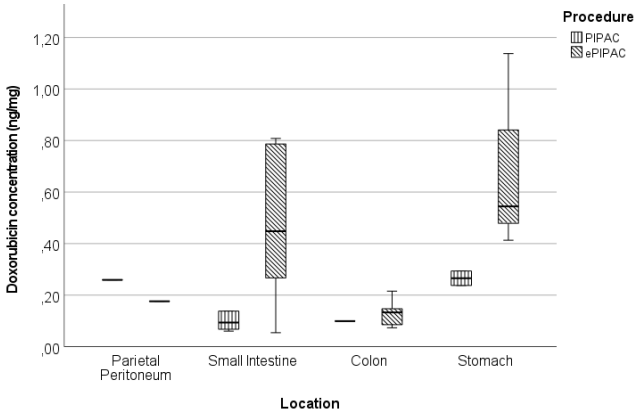

Figure 36. Median doxorubicin concentration after PIPAC vs ePIPAC among organs.

Mean doxorubicin concentration in the parietal peritoneum after PIPAC was 0.26ng/mg and ePIPAC 0.24±0.09ng/mg ($p>0.5$), in small intestine 0.10±0.037ng/mg and 0.70±0.77ng/mg ($p>0.05$), in colon 0.10ng/mg and 0.13±0.06ng/mg ($p>0.5$), in stomach 0.27±0.04ng/mg and 0.70±0.39ng/mg ($p>0.05$). The difference after PIPAC between the parietal peritoneum and small intestine, small

intestine and stomach was significant ($p<0.05$). No significance can be derived between the parietal peritoneum and colon because the drug concentration was below the sensitivity threshold in two of three probes from each region. No significant difference was found between the parietal peritoneum and the stomach, small intestine and colon, as well as between the colon and stomach ($p>0.05$). After ePIPAC, no significant difference was found between the parietal peritoneum and small intestine, parietal peritoneum and colon, parietal peritoneum and stomach, small intestine and colon ($p>0.05$), and small intestine and stomach ($p>0.5$). Lastly, the difference between the colon and stomach was significant ($p<0.05$).

ePIPAC on ex vivo Rabbit: spatial doxorubicin distribution over PIPAC

PIPAC had a significantly higher depth of doxorubicin penetration over ePIPAC, but the

standard deviation was lower in ePIPAC. Within the group, ePIPAC showed more homogeneous penetration than PIPAC.

ePIPAC vs PIPAC had no significant difference in doxorubicin concentration. The standard deviation was lower after PIPAC. Ultimately, doxorubicin distribution was more homogeneous in ePIPAC.

3.4.2 Enhanced Inverted Bovine Urinary Bladder

eIBUB comprises an inverted bovine urinary bladder connected with an airtight plastic box by the principle of communicating vessels. Both components are separately placed on scales. This setup allows over-time measurements of bladder weight and aerosol sedimentation. At the end of experiments, tissue biopsies can be taken for pharmacological studies.

3.4.2.1 Real-time tissue drug uptake

Aerosolization in eIBUB leads to tissue drug uptake with bladder weight increase, allowing calculation

of drug delivered to the tissue via weight difference before and after aerosolization.

ePIPAC for 6min delivered a higher drug volume than PIPAC for 36min and the same volume as ePIPAC for 10 and 30min. PIPAC for 36min delivered higher drug volume than ePIPAC for 36min. The difference among groups was not significant.

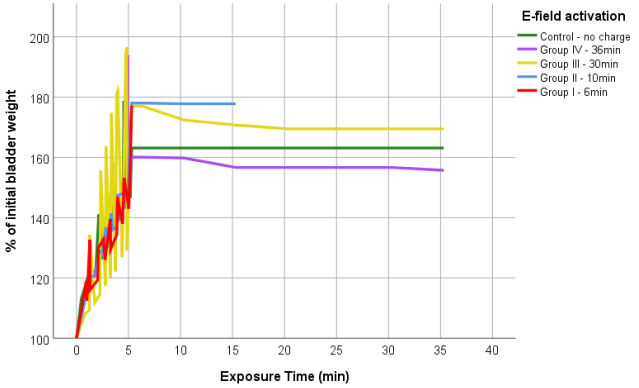

Figure 37. Overtime bladder weight after ePIPAC vs PIPAC.

Activation of electrostatic field (e-field): group I (red line): e-charge during aerosolization; group II (blue line): e-charge for 10min after aerosolization; group III (yellow line): e-charge for 30 min after aerosolization, group IV (purple line): e-charge during the whole experiment, control group (green line): 30min exposure after PIPAC, no e-charge.

Overtime bladder weight after ePIPAC and PIPAC is presented in Figure 37. In group I, mean relative bladder weight was 177.12±50.84%, in group II 177.89±38.92%, group III 171.88±30.08%, group IV 157.78±22.53% and in control 163.11±20.57%.

The difference between control and test, test and test, was not significant ($p>0.05$).

3.4.2.2 Real-time aerosol sedimentation

Aerosolization leads to sedimentation, which can be measured over time in eIBUB. The higher tissue drug uptake leads to lower sedimentation and vice versa.

ePIPAC for 6min had the lowest aerosol sedimentation vs PIPAC for 36min and ePIPAC for 10, 30 and 36min. PIPAC for 36min had the highest sedimentation. The difference between groups was not significant.

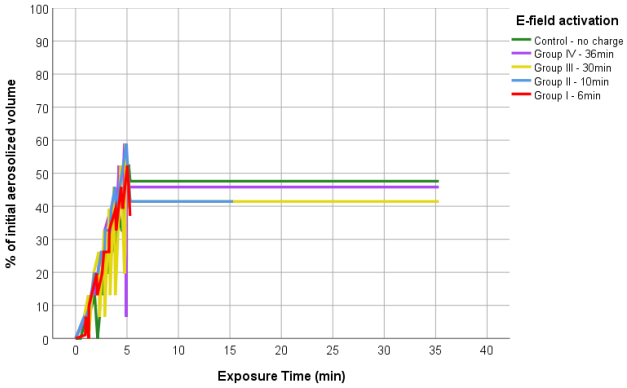

Figure 38. Overtime sedimented liquid during ePIPAC vs PIPAC.

Activation of electrostatic field (e-field): group I (red line): e-charge during aerosolization; group II (blue line): e-charge for 10min after aerosolization; group III (yellow line): e-charge for 30 min after aerosolization, group IV (purple line): e-charge during the whole experiment, control group (green line): 30min exposure after PIPAC, no e-charge.

Figure 38 represents the relative volume of sedimented aerosol. In group I, the volume was 37.09±32.28%, group II 41.45±30.74%, group III 41.45±17.55%, group IV 45.81±25.01%, and control 47.59±7.96%. The difference between

control and test, test and test, was not significant ($p>0.5$).

3.4.2.3 Depth of tissue penetration

The depth of doxorubicin penetration in eIBUB was measured qualitatively and quantitatively.

Complete tissue drug penetration was observed after ePIPAC in eIBUB groups III (30min exposure) and IV (36min exposure). Positive fluorescence in penetrated liquid was observed in all samples. The doxorubicin concentration in penetrated fluid in group III was 7659.67±4773.34ng/ml and cisplatin 50816.67±5068.89ng/ml. In group IV, the doxorubicin concentration was 1148.00±92.07ng/ml and cisplatin 50100.00±3451.09ng/ml. The wall thickness in group III was 5.89±1.05mm and in group IV, 4.67±1.58mm.

3.4.2.4 Drug tissue concentration

Doxorubicin tissue concentration was compared after 6, 10, 30 and 36min of ePIPAC and 36min of PIPAC – control.

ePIPAC for 6min had the highest tissue concentration over 10, 30, and 36min. The difference within the groups was not significant. PIPAC for 36min reached the same drug concentration as ePIPAC for 6min ($p>0.05$).

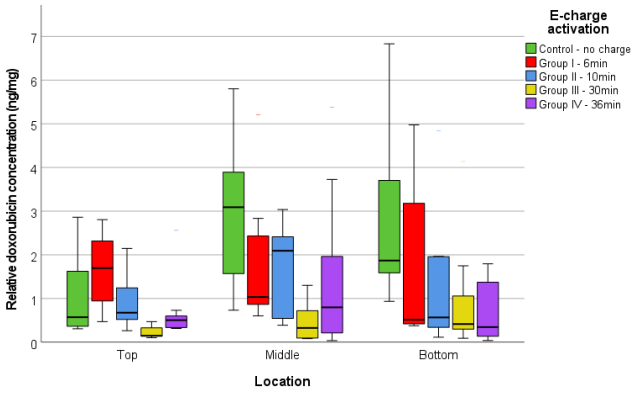

Figure 39. Median relative doxorubicin concentration at the top, middle and bottom of the enhanced inverted bovine urinary bladder after ePIPAC and PIPAC.

Green columns: control with no electrostatic charge; red columns: electrostatic precipitation for 6min during aerosolization; blue columns: electrostatic precipitation for 10min after aerosolization, yellow columns: electrostatic precipitation for 30min after aerosolization; purple columns: electrostatic precipitation during and after aerosolization for 36min.

Figure 39 demonstrates the median doxorubicin concentration in the eIBUB after PIPAC and ePIPAC. Four ePIPAC groups depending on application time were analyzed. In group I, the

electrostatic field was activated during aerosolization for 6min. The mean concentration of doxorubicin was at the top of the bladder 1.69±0.84ng/mg, in the middle 1.77±1.51ng/mg, and at the bottom 2.66±4.12ng/mg. In Group II, the electrostatic field was activated for 10min after aerosolization. The mean doxorubicin concentration at the top was 0.94±0.65ng/mg, in the middle 1.73±1.03ng/mg, and at the bottom 1.31±1.52ng/mg. In Group III, the electrostatic field was applied for 30min after aerosolization. The concentration at the top was 0.24±0.14ng/mg, in the middle 0.47±0.42ng/mg, and at the bottom 1.02±1.28ng/mg. In Group IV, the electrostatic field was applied for 36min before and after aerosolization. The concentration at the top was 0.71±0.71ng/mg, in the middle 1.62±1.83ng/mg, and at the bottom 0.68±0.74ng/mg. In the control group, no electrostatic field was applied. The concentration at the top was 1.08±0.97ng/mg, in the

middle 2.89±1.57ng/mg, and at the bottom 2.87±2.05ng/mg. The difference within all test groups was not significant ($p>0.05$) but in the control group between top and middle, top and bottom ($p<0.05$). At the top, a significant difference was observed between control and group III, groups I and II, groups I and III, groups I and IV, and groups II and III ($p<0.05$). In the middle of the bladder, the difference was significant between the control and group III, groups I and III, and groups II and III ($p<0.05$). At the bottom, significance was reached between the control and group III and IV ($p<0.05$).

The total doxorubicin concentration in group I was 2.04±2.52ng/mg, group II 1.33±1.13ng/mg, group III 0.58±0.82ng/mg, group IV 1.00±1.24ng/mg and control 2.28±1.76ng/mg. Statistical significance was between control and group I ($p=0.686$), control and group II ($p=0.022$), control and group III ($p<0.001$), and control and group IV ($p=0.003$).

3.4.2.5 ePIPAC application time: overview

ePIPAC for 6min showed the highest tissue drug uptake and the lowest aerosol sedimentation over all other groups. The doxorubicin concentration was the highest after 6 min ePIPAC than after 10, 30, and 36 min. There is no significant difference in total tissue drug uptake after 36min PIPAC and 6min ePIPAC. Drug distribution within ePIPAC groups was relatively homogeneous ($p>0.05$), but not within PIPAC. The doxorubicin penetration through the entire eIBUB wall over 4600µm was observed in ePIPAC groups III and IV.

In summary, 6min of ePIPAC delivers the highest volume of drugs within the shortest time with better homogeneity and deeper penetration than standard PIPAC for 36min.

4 Discussion

The presented work aims to provide a rationale combining PIPAC and electrostatic precipitation. This combination was analyzed in physical, in vitro, and ex vivo experiments, where application time, spatial drug distribution, and local toxicity were investigated. Results demonstrate that electrostatic precipitation can shorten PIPAC from 36min to 6min, leading to a shorter operation time, around 9 times higher penetration depth, more homogeneous drug distribution, and moderately enhanced cytotoxic activity. These findings have the potential to significantly improve the current therapeutic options for PM and open a new venue for preclinical and clinical studies.

ePIPAC is superior to PIPAC

Electrostatic precipitation improves the pharmacological properties of PIPAC. Electroporation occurs under high-voltage electric

impulses and leads to aqueous pore formation in the cell membrane, followed by increasing transmembrane transport of hydrophilic drugs [107]. This phenomenon was probably observed during ePIPAC by achieving meaningful tissue drug penetration while aerosolizing water-based substances. Moreover, irreversible electroporation might occur in some cells under high voltage, causing membrane instability and cell death, which can explain higher cell toxicity after ePIPAC vs PIPAC in some control groups. This effect is widely applied in oncology to enhance antitumor therapy. Another advantage of ePIPAC is more homogeneous drug distribution which could be explained by the precipitation of negatively charged aerosol to positively charged tissue.

Better therapeutic index (IP/IV)

Systemic drug bioavailability after ePIPAC is comparable with the direct intravenous drug

application. After systemic oxaliplatin administration of 130mg/m^2 in comparison to ePIPAC with 92mg/m^2, the mean plasma concentration after 24h ($AUC_{0\text{-}24h}$) was 54.8µg/ml*h for iv and 49.0-59.5µg/ml*h for intraperitoneal administration [93, 108]. Despite the lower dosage applied during ePIPAC, the plasma concentration was even higher than after the systemic administration. Some authors explained high drug bioavailability by a shorter application time during the ePIPAC. Additionally, two physical principles facilitate better drug distribution during ePIPAC: aerosol physical properties and electrostatic precipitation. The synergy of these physical effects can transport hydrophilic drugs, usually characterized by low penetration and bioavailability, deeper and more homogeneous into the target tissue. Another study reported rapid systemic drug absorption around four times in 20min after the release of capnoperitoneum [69]. The reperfusion

phenomenon might explain such absorption after venous decompression. It leads to quick tissue clearance and raises systemic concentration. A capnoperitoneum, therefore, might play an important role in maintaining tissue drug concentration and require further investigation. In our study, ePIPAC shows complete tissue drug penetration of around 4000µm in 30min with tissue drug absorption of 116ml. Furthermore, doxorubicin fluorescence was observed in the lumen of blood vessels on the outer bladder surface, proving ePIPAC as a high-volume drug delivery system with high tissue drug availability.

Shorter delivery time

Electrostatic precipitation has the potential to shorten PIPAC to 5 times. The exposure time of 30min after aerosolization, the current standard for PIPAC, caused full tissue drug penetration during ePIPAC on the eIBUB model, leading to droplets

forming outside of the bladder and decreased tissue drug concentration. On the contrary, ePIPAC for 6 min showed tissue drug delivery comparable to a PIPAC for 36 min with no significant difference in tissue drug concentration and more homogeneous distribution. Compared to a simple peritoneal lavage or HIPEC, ePIPAC can shorten the application time to 15 times. As a result, a shorter application time can reduce patients' surgery burden and recovery time.

Deeper tissue penetration

Electrostatic precipitation increases the depth of drug penetration. Although there was no significant difference in tissue aerosol absorption between ePIPAC and PIPAC, the depth of drug penetration is drastically different. By adding electrostatic precipitation, the penetration depth rises to 9 times and even exceeds the thickness of the target tissue. The possible explanation is aqueous pores form in

the cell membrane under the electrostatic field, allowing better drug tissue penetration. By comparing ePIPAC with peritoneal lavage or HIPEC, other local approaches in PM therapy, the drug penetration was 130 times higher. Clinically, increased penetration enhances tissue exposure to therapeutics and thus can improve tumor response rate. The drug penetration in ePIPAC depends on exposure time, so the depth can be adjusted to tumor or tissue thickness and size, opening windows to more personalized treatments.

Better homogeneity

The homogeneity of drug tissue distribution, defined as penetration depth and drug concentration in the tissue, was higher after ePIPAC compared to PIPAC. ePIPAC showed drastically higher penetration depth than PIPAC and HIPEC or peritoneal lavage, and the target tissue was saturated entirely with applied substances along the whole

thickness, which was not the case in other procedures. The drug tissue concentration has a narrower variance in ePIPAC with prolonged exposure time. Although 6min ePIPAC has no significant difference in drug tissue concentration compared to 36min PIPAC, the variance in drug concentration at the top, middle, and bottom of the bladder was higher than in ePIPAC for 30 and 36min. We assume that electrostatic precipitation improves the homogeneity of drug distribution in all three directions along axes x, y, and z. This assumption also clarifies why longer exposure time leads to lower drug concentration and decreased tissue weight. If axe y is equivalent to the vertical bladder surface, axe x corresponds to the horizontal surface and axe z describes the wall thickness, the longest axe would be y, then x, and the shortest one z. If we put all three axes in the time frame, axe z would be crossed at some time, probably faster than axes x and y, leading to a complete drug penetration

through the bladder wall with a decrease in tissue drug concentration.

This is a simplified model, where the influence of many other forces and their interactions were not entirely considered. For instance, gravity with higher potential than electrostatic force will pull the interstitial fluid along axes y, creating a gradient from top to bottom. Moreover, gravity enhances the sedimentation of inhomogeneous aerosol particles leading to liquid formation. Electrostatic precipitation can hardly overcome the high kinetic force of aerosol particles supported by gravity. Thus, the aerosolization angle mainly determines drug distribution. Theoretically, if the kinetic force of aerosol particles decreased enough, the electrostatic force could more homogeneously spread these particles in all directions, further improving the distribution. Perhaps, this process is ongoing during aerosolization involving the smallest and lightest aerosol particles and leading to considerable drug

penetration observed at the furthest point from the spray nozzle in the ex vivo model.

Enhanced biological effect(s)

Electrostatic precipitation moderately enhanced PIPAC antitumor activity. The apoptotic cell number immediately after treatment was higher in ePIPAC vs PIPAC. However, the number was lower after 24h with no significant difference between the groups. Such difference might be conditioned by reversible cell electroporation after ePIPAC, which reduces cell viability but does not lead a cell to death. Another point is reversible apoptosis. Some authors reported that cells retain the possibility of recovering after a cytotoxic substance was washed out and a cell medium was added [109]. We assume that reversible electroporation might induce reversible apoptosis observed immediately after treatment.

Cell viability 48h after the treatment was significantly lower in ePIPAC control vs PIPAC control, which might be due to an additional cytotoxic effect of electrostatic precipitation. The same tendency was observed in the cell growth inhibition study showing impaired cell growth in the ePIPAC control group. Increased cell toxicity in the ePIPAC control group might result from irreversible cell electroporation leading to cell membrane instability and irreversible apoptosis. After ePIPAC on eIBUB, the number of cleaved caspase-3 positive cells was significantly higher than in the control. However, no significant difference was found in comparison to PIPAC. Such results might be due to low cell vitality or metabolic activity in the ex vivo model or to the short time between the end of therapy and biopsies. At the same time, longer exposure is associated with apoptosis even without treatment, determined by the biodegradation of avascularised tissue.

Indeed, when there is no difference in cleaved caspase-3 after ePIPAC and PIPAC, higher cell toxicity under electrostatic precipitation can be induced by another mechanism not elucidated in our study or for unknown reasons. Moreover, cleaved caspase activity was measured in an ex vivo model, which might have significant differences compared to in vitro or in vivo models. Thus, there is a need for further investigations focused on the antitumor activity of ePIPAC.

Higher tissue concentration

There was no difference in tissue drug concentration between PIPAC and 6min ePIPAC in the bovine urinary bladder model. However, over time, liquid drag through the eIBUB wall was observed in the ePIPAC group, leading to lower tissue drug concentration and diminished weight, meaning that the thickness of the tissue influences drug penetration and tissue drug concentration. From

another point of view, drug delivery occurs during aerosolization with an increase in bladder weight without immediate complete tissue drug penetration. It means that aerosol oversaturates the superficial layers of target tissue even under electrostatic precipitation, which leads to aerosol sedimentation and liquid formation. During the exposure time, the liquid is transported by electrostatic precipitation through the entire wall causing complete tissue drug penetration. By reducing the velocity of aerosolization, the hydrostatic tissue pressure might be overcome by electrostatic precipitation dragging liquid deeper through the layers, which might increase the tissue drug concentration, reduce the volume of sedimented aerosol and, as a result, improve the efficiency of aerosol chemotherapy.

Aerosol physical properties

Many factors influence aerosol chemotherapy, like aerosol diameter, droplet size distribution, kinetic force, and angle of aerosolization.

It is known that a smaller droplet size of 1-5μm has the best distribution in a given volume [110]. However, generating an aerosol with such a narrow distribution is quite demanding. Market-available spray nozzle Capnopen® produces an aerosol with a distribution size from 22μm to 144μm. Considering the significant mass difference, the kinetic force of these droplets will strongly vary, influencing the particles' velocity. Furthermore, the large particles will be most affected by the force of gravity, which further increases sedimentation.

Increasing the space among particles or changing their direction may prevent their growth. We observed a stable aerosol fraction in the plastic box model after adding electrostatic precipitation. By

avoiding the growth of the fine aerosol fraction, drug distribution can be significantly improved. Small particles have the lowest kinetic force, and thus their direction might be changed by electrostatic precipitation. The Belgic group showed better ink staining of the swine tissue placed behind the spray nozzle by adding electrostatic precipitation to PIPAC. Possibly, this effect was caused by the fine droplet fraction, which was dragged under electrostatic force against gravity. In our eIBUB study, the drug tissue concentration was the highest at the top after 6min ePIPAC, creating a gradient to the bottom. This also might be preconditioned by the location of the active electrode at the top of the bladder.

Nonetheless, the droplets with higher mass cannot be redirected by the electric force. In the eIBUB, electric force distributes through the whole organ with a higher gradient near electrodes. It means that the sedimentation of larger aerosol particles will be

rather accelerated by electrostatic force with neglectable changes in direction. Hence, the distribution for such particles will depend mainly on the spray angle. In the Capnopen®, the spray angle increases by higher spray flow, which from the one side, raises the area of exposure and, from the other side, further accelerates the velocity, which can negatively affect the distribution of the fine fraction. From our perspective, the fine fraction is responsible for drug delivery to the furthest and the most hidden parts of the abdominal cavity. Thus, the balance between injection flow, angle, and distribution must be found. In 2D and 3D blotting paper models, ink distribution was inhomogeneous for both PIPAC and ePIPAC. Furthermore, PIPAC demonstrated an even better distribution than ePIPAC, which might be explained by the prevalence of high-volume aerosol fraction, which has a lower floating time and tends to sediment more quickly under electrostatic force. Moreover, the shape of the 3D model might

influence the distribution because the distance between the spray nozzle and surface is the shortest in the middle of the conic paper (zone 2), then in the cone base.

Although the computation modelling applied by the Belgic group has many benefits, such as cost-effectiveness and applicability, a significant difference was observed compared to experimental models, especially in the "problem areas" behind the spray nozzle, where the distribution has to be improved. Thus, the need for a real-life experimental model remains high. Notwithstanding, computation modelling might have an important role in experiment planning and hypothesizing.

Local cell toxicity

The effectiveness of PIPAC in inducing cell apoptosis was demonstrated by the French research group of Marc Pocard [111]. In our study, we further compared local cell toxicity between PIPAC and

ePIPAC, where electrostatic precipitation moderately improved the cytotoxic effect. Electroporation might be responsible for such results. Aqueous pores appear in the cell membrane under high-frequency electric impulses, allowing hydrophilic drugs to penetrate deeper into the tissue [107]. Moreover, instability of the cell membrane might directly induce irreversible apoptosis leading to programmed cell death. As most drugs applied intraperitoneally are hydrophilic, the enhancement of drug penetration and distribution is highly expected in ePIPAC. Although ePIPAC enhances cell toxicity, no difference in cleaved caspase-3 was observed compared to PIPAC. It might be another mechanism that predefines the effect of ePIPAC, which requires further investigation.

Ex vivo pharmacological studies

The concentration of oxaliplatin in the swine model was compared by Giger Pabst after PIPAC and

ePIPAC. Significantly lower drug concentration was observed in visceral organs compared to parietal ones after both procedures [69]. The same tendency was observed by Axel Davigo after PIPAC with cisplatin [112]. Although the visceral peritoneum is larger than the parietal one, the drug availability is low. In our study, PIPAC and ePIPAC were conducted on a post-mortem rabbit model, where after ePIPAC no significant difference between parietal and visceral organs was observed.

Moreover, the mean doxorubicin concentration after ePIPAC was meaningfully higher than after PIPAC. The difference might be explained by anatomical differences between swine and rabbits and by different drugs. Another point is the absence of blood circulation without drug clearance from the tissue. Nonetheless, these findings again show the need to establish drug-device combinations.

In the eIBUB model, doxorubicin concentration was the highest at the top after 6min ePIPAC and the lowest after 36min PIPAC. The same tendency was demonstrated by Giger Pabst in a swine model, where adding electrostatic precipitation reduced the tissue concentration in the parietal peritoneum, making different points more comparable with each other. The decrease in tissue drug concentration in ePIPAC may be explained by enhanced tissue drug penetration observed in eIBUB, where therapeutics are dragged under an electrostatic field deeper into or even through the tissue, which leads to overtime lowering of the drug concentration and tissue liquid saturation. Hence, the depth of tumor penetration depends on the thickness of the tissue and can be adjusted by exposure time.

In conclusion, ePIPAC is a high-volume drug delivery system becoming an attractive alternative for current treatment options in PM. ePIPAC can deliver solutions with different viscosity, and

chemical, physical and biological properties opening the window for personalized use.

ePIPAC not only improves aerosol properties but, modifies target tissue, for example, creating aqueous pores and reducing interstitial fluid pressure. All of this led to higher tissue drug penetration and more homogeneous drug distribution. Moreover, the application time can be considerably shortened by electrostatic precipitation. By modifying application time, the depth of drug penetration might be adjusted to tumor thickness optimizing tumor exposure to drugs. Additionally, the depth of drug penetration can be modified by changing the polarity of the electrostatic charge, which will drag the substance in the opposite direction. The effect of electrostatic precipitation might be further enhanced by charged drug carriers such as nanoparticles.

The additional local cytotoxic effect of electrostatic precipitation intensifies the direct tumor damage

allowing lower cytotoxic drug dosing. Therefore, systemic toxicity and drug-related side effects might be diminished.

The homogeneity of spatial drug distribution increases under electrostatic precipitation, which can overcome pharmacological differences between the visceral and parietal peritoneum.

The minimally invasive approach and the short application time can further extend the indication of ePIPAC in an outpatient setting. For instance, repetitive aerosol chemotherapy can be conducted in whole organs such urinary bladder, stomach, or esophagus. In addition, the well-established eIBUB model can be widely used to optimize the treatment of urothelial diseases. Furthermore, the combination of endoluminal and intraabdominal chemotherapies might help to achieve the best tumor exposure and response.

Finally, electrostatic precipitation can improve occupational safety by reducing application and working time in the operating room. All mentioned benefits of ePIPAC positively affect therapy costs and applicability.

The following research aspects were investigated in this work:

- ePIPAC is superior to PIPAC

ePIPAC can shorten PIPAC from 36min to 6min by delivering the same drug volume into the target tissue. The size distribution and floating time of aerosol particles are lower in ePIPAC vs PIPAC. Electrostatic precipitation itself showed a moderate cytotoxic effect which might enhance antitumor activity. Although the tissue drug concentration was the same after ePIPAC vs PIPAC, the depth of tissue drug penetration was significantly higher during ePIPAC. The last confirms more homogenous drug distribution after ePIPAC.

- Better therapeutic index (IP/IV)

Systemic drug concentration after ePIPAC is not inferior to direct intravenous drug application. High drug bioavailability in ePIPAC is determined by aerosol physical properties, leading to homogeneous drug distribution and high tissue drug absorption. Under electrostatic precipitation, the drugs are transferred more profoundly into the tissue, reaching and penetrating the vascular net. Furthermore, the application time of ePIPAC is significantly shorter than intravenous application, which reduces the time for drug clearance.

- Shorter delivery time

ePIPAC for 6min delivers the same volume of therapeutics as PIPAC for 36min. There is no significant difference between the stated groups in tissue aerosol absorption and aerosol sedimentation. Moreover, a longer exposure time in ePIPAC led to

full liquid penetration through the target tissue and a weight decrease.

- Deeper tissue penetration

In ePIPAC, the depth of tissue drug penetration was nine times higher than in PIPAC and equal to 4000μm. Complete tissue drug penetration was seen in the ePIPAC groups with 30min and 36min exposure, but not in PIPAC.

- Higher tissue concentration

There was no significant difference in tissue drug concentration after 6min ePIPAC and 36min PIPAC. The longer exposure time in ePIPAC led to decreased tissue drug concentration.

- Better homogeneity

Drug distribution was more homogeneous in ePIPAC vs PIPAC, which was evaluated based on the tissue drug concentration and depth of tissue drug penetration.

- Enhanced biological effect(s)

ePIPAC showed moderately higher local toxicity compared to PIPAC. After treatment, the number of apoptotic cells was higher after ePIPAC vs PIPAC, and cell viability in 48h was respectively lower.

Further development

Despite of wide application of ePIPAC, there are many points for further development, such as optimizing the position of spray nozzle and flow, establishing drug-device combinations based on tumor biology, and investigating the influence of electrostatic precipitation on hydrostatic tissue pressure.

5 Summary

Pressurized Intraperitoneal Aerosol Chemotherapy (PIPAC) is a minimally invasive local laparoscopic procedure for treating peritoneal malignancies. Electrostatic precipitation was combined with PIPAC (ePIPAC) to further improve the homogeneity of drug distribution. Under high voltage, aqueous pores appear in the cell membrane leading to higher drug penetration. This process is called electroporation and is widely applied in oncology. Furthermore, electroporation might induce irreversible cell membrane damage, increasing the antitumor effect. Although ePIPAC is already implemented in clinical studies, preclinical data are modest. For instance, the application time is not well established, but according to recent research might play an important role in tumor response to therapy.

In this study, we provided a preclinical background for ePIPAC, where aerosol distribution and sedimentation were investigated in real-time in physical experiments, local toxicity in cell culture model, spatial tissue drug distribution, real-time aerosol absorption, and sedimentation were analyzed in ex vivo models. The influence of application time on tissue drug distribution was complementarily shown.

By adding electrostatic precipitation to PIPAC, the floating time of aerosol was less than 25sec after aerosolization, and the median aerosol diameter of the fine fraction, which is responsible for deeper and more homogeneous tissue drug penetration, was stable. In vitro, ePIPAC showed enhanced antitumor activity compared to PIPAC, with a higher number of apoptotic cells right after the treatment and lower cell metabolic activity after 48h. Both procedures inhibit cell growth entirely on day nine after the treatment. In the ex vivo enhanced inverted bovine

urinary bladder model (eIBUB), ePIPAC delivered over 100ml of therapeutics within 6min, which was comparable with PIPAC for 36min. However, the spatial drug distribution was more homogeneous after ePIPAC vs PIPAC. Increasing exposure time to 30min led to tissue drug penetration over 4000µm in ePIPAC, versus around 500µm during PIPAC. Moreover, more intense cleaved caspase-3 staining was in the outer layers of eIBUB after ePIPAC, which might confirm a higher apoptosis rate compared to PIPAC. The ex vivo rabbit model showed the same patterns in tissue drug distribution as eIBUB. The tissue drug concentration was higher in visceral organs after ePIPAC vs PIPAC.

In conclusion, ePIPAC allows more homogeneous and deeper tissue drug distribution than PIPAC, with slightly enhanced in vitro toxicity. Ex vivo, ePIPAC had 5 times shorter application time than PIPAC with more intense apoptosis staining in the deeper layers.

The further optimization of ePIPAC requires in vivo studies on a large healthy animal model, e.g. swine, where spatial drug distribution, systemic drug clearance, and toxicity have to be evaluated.

By confirming our results, the application time of PIPAC can be reduced with more homogenous drug distribution and higher local toxicity. All this might improve outcomes and the quality of patients' life affected by peritoneal malignancies.

5.1 Summary (German translation)

Die “Pressurized IntraPeritoneal Aerosol Chemotherapy” (PIPAC) ist ein minimalinvasives lokales laparoskopisches Verfahren zur Behandlung von bösartigen Erkrankungen des Peritoneums. Elektrostatische Fällung wurde mit der PIPAC (ePIPAC) kombiniert, um die Homogenität der Arzneimittelverteilung weiter zu verbessern. Unter Hochspannung entstehen wässrige Poren in der Zellmembran, die zu einer höheren Wirkstoffpenetration führen. Dieser Prozess wird Elektroporation genannt und findet in der Onkologie breite Anwendung. Darüber hinaus könnte die Elektroporation zu einer irreversiblen Schädigung der Zellmembran führen und so die Antitumorwirkung verstärken. Obwohl ePIPAC bereits in klinischen Studien eingesetzt wird, sind die präklinischen Daten bescheiden. Beispielsweise ist die Anwendungsdauer nicht genau bekannt, aber neueren Forschungsergebnissen zufolge könnte sie

eine wichtige Rolle für das Ansprechen des Tumors auf die Therapie spielen.

In dieser Studie lieferten wir einen präklinischen Hintergrund für ePIPAC, bei dem die Aerosolverteilung und -sedimentation in Echtzeit in physikalischen Experimenten untersucht, die lokale Toxizität im Zellkulturmodell, die räumliche Arzneimittelverteilung im Gewebe sowie die Aerosolabsorption und -sedimentation in Echtzeit in ex vivo Modellen analysiert wurden. Ergänzend wurde der Einfluss der Anwendungszeit auf die Arzneimittelverteilung im Gewebe gezeigt.

Durch die Zugabe von elektrostatischer Fällung zur PIPAC betrug die Schwebezeit des Aerosols weniger als 25 Sekunden nach der Aerosolisierung, und der median Aerosoldurchmesser der Feinfraktion, der für eine tiefere und homogenere Wirkstoffpenetration im Gewebe verantwortlich ist, war stabil. In vitro zeigte ePIPAC im Vergleich zu

PIPAC eine erhöhte Antitumoraktivität, mit einer höheren Anzahl apoptotischer Zellen direkt nach der Behandlung und einer geringeren Zellstoffwechselaktivität nach 48 Stunden. Beide Verfahren hemmen das Zellwachstum am neunten Tag nach der Behandlung vollständig. Im ex vivo verstärkten invertierten Rinderharnblasenmodell (eIBUB) lieferte ePIPAC über 100 ml Therapeutika innerhalb von 6 Minuten, was mit PIPAC für 36 Minuten vergleichbar war. Jedoch war die räumliche Arzneimittelverteilung nach ePIPAC vs PIPAC homogener. Eine Erhöhung der Expositionszeit auf 30 Minuten führte bei der ePIPAC zu einer Gewebepenetration von Arzneimitteln über 4000 µm, gegenüber etwa 500 µm bei der PIPAC. Darüber hinaus zeigten die äußeren Schichten von eIBUB nach ePIPAC eine intensivere Färbung bezüglich gespaltener Caspase-3, was eine höhere Apoptoserate im Vergleich zu PIPAC bestätigen könnte. Das ex vivo Kaninchenmodell zeigte die

gleichen Muster bei der Arzneimittelverteilung im Gewebe wie eIBUB. Die Gewebekonzentration des Arzneimittels war in den viszeralen Organen nach ePIPAC höher als nach PIPAC

Zusammenfassend lässt sich sagen, dass ePIPAC eine homogenere und tiefere Arzneimittelverteilung im Gewebe als PIPAC ermöglicht, mit leicht erhöhter in vitro Toxizität. Ex vivo hatte ePIPAC eine fünfmal kürzere Anwendungszeit als PIPAC und eine intensivere Apoptosefärbung in den tieferen Schichten.

Die weitere Optimierung von ePIPAC erfordert in vivo Studien an einem großen gesunden Tiermodell, z.B. Schweine, bei denen die räumliche Arzneimittelverteilung, die systemische Arzneimittelclearance und die Toxizität bewertet werden müssen.

Durch die Bestätigung unserer Ergebnisse kann die Anwendungszeit von PIPAC verkürzt werden, was

zu einer homogeneren Arzneimittelverteilung und einer höheren lokalen Toxizität führt. All dies könnte die Ergebnisse und die Lebensqualität von Patienten verbessern, die von peritonealen Malignomen betroffen sind.

6 List of References

1. Bichat M, *Treatise on the Membranes in general, and on different Membranes in particular*. A new edition ed. Vol. 1. 1813, Boston: Cummings and Hilliard. 79-83.
2. Albanese AM, Albanese EF, Miño JH, Gómez E, Gómez M, Zandomeni M, and Merlo AB, *Peritoneal surface area: measurements of 40 structures covered by peritoneum: correlation between total peritoneal surface area and the surface calculated by formulas.* Surg Radiol Anat, 2009. **31**(5): p. 369-77.
3. Redlarski G, Palkowski A, and Krawczuk M, *Body surface area formulae: an alarming ambiguity.* Scientific Reports, 2016. **6**(1): p. 27966.
4. Reymond MA, *Pleura and Peritoneum: the forgotten organs.* Pleura and peritoneum, 2016. **1**(1): p. 1-2.
5. Blackburn SC and Stanton MP, *Anatomy and physiology of the peritoneum.* Seminars in Pediatric Surgery, 2014. **23**(6): p. 326-330.
6. Michailova KN and Usunoff KG, *Serosal membranes (pleura, pericardium, peritoneum). Normal structure, development and experimental pathology.* Adv Anat Embryol Cell Biol, 2006. **183**: p. i-vii, 1-144, back cover.
7. Solass W, Horvath P, Struller F, Königsrainer I, Beckert S, Königsrainer A, Weinreich F-J, and

Schenk M, *Functional vascular anatomy of the peritoneum in health and disease.* Pleura and peritoneum, 2016. **1**(3): p. 145-158.
8. Struller F, Weinreich FJ, Horvath P, Kokkalis MK, Beckert S, Königsrainer A, and Reymond MA, *Peritoneal innervation: embryology and functional anatomy.* Pleura Peritoneum, 2017. **2**(4): p. 153-161.
9. diZerega GS and Campeau JD, *Peritoneal repair and post-surgical adhesion formation.* Hum Reprod Update, 2001. **7**(6): p. 547-55.
10. Gautam A, Park BK, Kim TH, Akauliya M, Kim D, Maharjan S, Park J, Kim J, Lee H, Park M-S, Lee Y, and Kwon H-J, *Peritoneal Cells Mediate Immune Responses and Cross-Protection Against Influenza A Virus.* 2019. **10**(1160).
11. Park JH, Kim YG, Shaw M, Kanneganti TD, Fujimoto Y, Fukase K, Inohara N, and Núñez G, *Nod1/RICK and TLR signaling regulate chemokine and antimicrobial innate immune responses in mesothelial cells.* J Immunol, 2007. **179**(1): p. 514-21.
12. Turyna B, Jurek A, Gotfryd K, Siaśkiewicz A, Kubit P, and Klein A, *Peritonitis-induced antitumor activity of peritoneal macrophages from uremic patients.* Folia Histochem Cytobiol, 2004. **42**(3): p. 147-53.
13. Sugarbaker PH, *Peritoneum as the first-line of defense in carcinomatosis.* J Surg Oncol, 2007. **95**(2): p. 93-6.

14. Gotloib L, Bar Sella P, Jaichenko J, and Shustack A, *Ruthenium-red-stained polyanionic fixed charges in peritoneal microvessels.* Nephron, 1987. **47**(1): p. 22-8.
15. *How does dialysis work?* 2006 [cited 12.05. 2021]; Available from: https://www.ncbi.nlm.nih.gov/books/NBK492981/.
16. Wassilev W, Wedel T, Michailova K, and Kühnel W, *A scanning electron microscopy study of peritoneal stomata in different peritoneal regions.* Ann Anat, 1998. **180**(2): p. 137-43.
17. Dedrick RL, Myers CE, Bungay PM, and DeVita VT, Jr., *Pharmacokinetic rationale for peritoneal drug administration in the treatment of ovarian cancer.* Cancer Treat Rep, 1978. **62**(1): p. 1-11.
18. De Smet L, Ceelen W, Remon JP, and Vervaet C, *Optimization of drug delivery systems for intraperitoneal therapy to extend the residence time of the chemotherapeutic agent.* TheScientificWorldJournal, 2013. **2013**: p. 720858-720858.
19. Goffin E, *Peritoneal membrane structural and functional changes during peritoneal dialysis.* Semin Dial, 2008. **21**(3): p. 258-65.
20. Rippe B, Stelin G, and Haraldsson B, *Computer simulations of peritoneal fluid transport in CAPD.* Kidney International, 1991. **40**(2): p. 315-325.
21. Reymond MA, *Definition and semantics: "Peritoneal Carcinomatosis" should be*

abandoned and replaced by "Peritoneal Metastasis". Pleura and peritoneum, 2017. **2**(3): p. 119-120.

22. Sugarbaker PH, *Pharmacology of chemotherapy treatments for peritoneal metastases: optimizing and augmenting HIPEC.* Pleura and peritoneum, 2017. **2**(2): p. 43-45.
23. Solon JG, O'Neill M, Chang KH, Deady S, Cahill R, Moran B, Shields C, and Mulsow J, *An 18 year population-based study on site of origin and outcome of patients with peritoneal malignancy in Ireland.* European Journal of Surgical Oncology (EJSO), 2017. **43**(10): p. 1924-1931.
24. del Castillo CF and Warshaw L, *Peritoneal metastases in pancreatic carcinoma.* Hepatogastroenterology, 1993. **40**(5): p. 430-2.
25. Schmidt S, Meuli RA, Achtari C, and Prior JO, *Peritoneal Carcinomatosis in Primary Ovarian Cancer Staging: Comparison Between MDCT, MRI, and 18F-FDG PET/CT.* Clinical Nuclear Medicine, 2015. **40**(5).
26. Flanagan M, Solon J, Chang KH, Deady S, Moran B, Cahill R, Shields C, and Mulsow J, *Peritoneal metastases from extra-abdominal cancer – A population-based study.* European Journal of Surgical Oncology, 2018. **44**(11): p. 1811-1817.
27. Quere P, Facy O, Manfredi S, Jooste V, Faivre J, Lepage C, and Bouvier AM, *Epidemiology, Management, and Survival of Peritoneal Carcinomatosis from Colorectal Cancer: A*

Population-Based Study. Dis Colon Rectum, 2015. **58**(8): p. 743-52.

28. Thomassen I, van Gestel YR, van Ramshorst B, Luyer MD, Bosscha K, Nienhuijs SW, Lemmens VE, and de Hingh IH, *Peritoneal carcinomatosis of gastric origin: a population-based study on incidence, survival and risk factors.* Int J Cancer, 2014. **134**(3): p. 622-8.
29. Hentzen JEKR, Rovers KP, Kuipers H, van der Plas WY, Been LB, Hoogwater FJH, van Ginkel RJ, Hemmer PHJ, van Dam GM, de Hingh IHJT, and Kruijff S, *Impact of Synchronous Versus Metachronous Onset of Colorectal Peritoneal Metastases on Survival Outcomes After Cytoreductive Surgery (CRS) with Hyperthermic Intraperitoneal Chemotherapy (HIPEC): A Multicenter, Retrospective, Observational Study.* Annals of surgical oncology, 2019. **26**(7): p. 2210-2221.
30. Yamagata K, Kumagai K, Shimizu K, Masuo K, Nishida Y, and Yasui A, *Gastrointestinal Cancer Metastasis and Lymphogenous Spread: Viewpoint of Animal Models of Lymphatic Obstruction.* Japanese Journal of Clinical Oncology, 1998. **28**(2): p. 104-106.
31. Wong SY and Hynes RO, *Lymphatic or hematogenous dissemination: how does a metastatic tumor cell decide?* Cell cycle (Georgetown, Tex.), 2006. **5**(8): p. 812-817.
32. Zoetmulder F, *Peritoneal Carcinomatosis of Colorectal Cancer*, in *Intraperitoneal Cancer*

Therapy, C. Helm and R. Edwards, Editors. 2007, Humana Press: Totowa, NJ, USA. p. 119.

33. Glockzin G and Piso P, *Current Statis and Future Directions in Gastric Cancer with Peritoneal Dissemenation*, in *Surgical Oncology Clinics of North America*, N. Petrelli, Editor. 2012, Saunders an imprint of ELSEVIER: Philadelphia, USA. p. 626.
34. Franke AJ, Iqbal A, Starr JS, Nair RM, and George TJ, *Management of Malignant Bowel Obstruction Associated With GI Cancers.* Journal of Oncology Practice, 2017. **13**(7): p. 426-434.
35. Klaver CEL, Groenen H, Morton DG, Laurberg S, Bemelman WA, Tanis PJ, and the research committee of the European Society of C, *Recommendations and consensus on the treatment of peritoneal metastases of colorectal origin: a systematic review of national and international guidelines.* Colorectal Disease, 2017. **19**(3): p. 224-236.
36. Palumbo MO, Kavan P, Miller WH, Jr., Panasci L, Assouline S, Johnson N, Cohen V, Patenaude F, Pollak M, Jagoe RT, and Batist G, *Systemic cancer therapy: achievements and challenges that lie ahead.* Frontiers in pharmacology, 2013. **4**: p. 57-57.
37. Francescutti V, Rivera L, Seshadri M, Kim M, Haslinger M, Camoriano M, Attwood K, Kane JM, 3rd, and Skitzki JJ, *The benefit of intraperitoneal chemotherapy for the*

treatment of colorectal carcinomatosis. Oncology reports, 2013. **30**(1): p. 35-42.

38. Casper ES, Kelsen DP, Alcock NW, and Lewis JL, Jr., *Ip cisplatin in patients with malignant ascites: pharmacokinetic evaluation and comparison with the iv route.* Cancer Treat Rep, 1983. **67**(3): p. 235-8.
39. Yu P, Ye Z, Dai G, Zhang Y, Huang L, Du Y, and Cheng X, *Neoadjuvant systemic and hyperthermic intraperitoneal chemotherapy combined with cytoreductive surgery for gastric cancer patients with limited peritoneal metastasis: a prospective cohort study.* BMC Cancer, 2020. **20**(1): p. 1108.
40. van Driel WJ, Koole SN, Sikorska K, Schagen van Leeuwen JH, Schreuder HWR, Hermans RHM, de Hingh I, van der Velden J, Arts HJ, Massuger L, Aalbers AGJ, Verwaal VJ, Kieffer JM, Van de Vijver KK, van Tinteren H, Aaronson NK, and Sonke GS, *Hyperthermic Intraperitoneal Chemotherapy in Ovarian Cancer.* N Engl J Med, 2018. **378**(3): p. 230-240.
41. Bakrin N, Bereder JM, Decullier E, Classe JM, Msika S, Lorimier G, Abboud K, Meeus P, Ferron G, Quenet F, Marchal F, Gouy S, Morice P, Pomel C, Pocard M, Guyon F, Porcheron J, and Glehen O, *Peritoneal carcinomatosis treated with cytoreductive surgery and Hyperthermic Intraperitoneal Chemotherapy (HIPEC) for advanced ovarian carcinoma: a French multicentre retrospective cohort study*

of 566 patients. Eur J Surg Oncol, 2013. **39**(12): p. 1435-43.

42. Hotouras A, Desai D, Bhan C, Murphy J, Lampe B, and Sugarbaker PH, *Heated IntraPEritoneal Chemotherapy (HIPEC) for Patients With Recurrent Ovarian Cancer: A Systematic Literature Review.* Int J Gynecol Cancer, 2016. **26**(4): p. 661-70.
43. Seshadri RA and Glehen O, *Cytoreductive surgery and hyperthermic intraperitoneal chemotherapy in gastric cancer.* World J Gastroenterol, 2016. **22**(3): p. 1114-30.
44. Polanco PM, Ding Y, Knox JM, Ramalingam L, Jones H, Hogg ME, Zureikat AH, Holtzman MP, Pingpank J, Ahrendt S, Zeh HJ, Bartlett DL, and Choudry HA, *Outcomes of Cytoreductive Surgery and Hyperthermic Intraperitoneal Chemoperfusion in Patients with High-Grade, High-Volume Disseminated Mucinous Appendiceal Neoplasms.* Ann Surg Oncol, 2016. **23**(2): p. 382-90.
45. Liu Y, Ishibashi H, Takeshita K, Mizumoto A, Hirano M, Sako S, Takegawa S, Takao N, Ichinose M, and Yonemura Y, *Cytoreductive Surgery and Hyperthermic Intraperitoneal Chemotherapy for Peritoneal Dissemination from Small Bowel Malignancy: Results from a Single Specialized Center.* Ann Surg Oncol, 2016. **23**(5): p. 1625-31.
46. Collaborators ICON, *International Collaborative Ovarian Neoplasm Trial 1: A Randomized Trial*

of Adjuvant Chemotherapy in Women With Early-Stage Ovarian Cancer. JNCI: Journal of the National Cancer Institute, 2003. **95**(2): p. 125-132.

47. Earle CC and Maroun JA, *Adjuvant chemotherapy after curative resection for gastric cancer in non-Asian patients: revisiting a meta-analysis of randomised trials.* Eur J Cancer, 1999. **35**(7): p. 1059-64.
48. Knight G, Earle CC, Cosby R, Coburn N, Youssef Y, Malthaner R, and Wong RK, *Neoadjuvant or adjuvant therapy for resectable gastric cancer: a systematic review and practice guideline for North America.* Gastric Cancer, 2013. **16**(1): p. 28-40.
49. Franko J, Shi Q, Goldman CD, Pockaj BA, Nelson GD, Goldberg RM, Pitot HC, Grothey A, Alberts SR, and Sargent DJ, *Treatment of colorectal peritoneal carcinomatosis with systemic chemotherapy: a pooled analysis of north central cancer treatment group phase III trials N9741 and N9841.* Journal of clinical oncology : official journal of the American Society of Clinical Oncology, 2012. **30**(3): p. 263-267.
50. Franko J, *Therapeutic efficacy of systemic therapy for colorectal peritoneal carcinomatosis: Surgeon's perspective.* Pleura Peritoneum, 2018. **3**(1): p. 20180102.
51. Sugarbaker PH, *Prevention and Treatment of Peritoneal Metastases: a Comprehensive*

Review. Indian J Surg Oncol, 2019. **10**(1): p. 3-23.

52. Mehta SS, Bhatt A, and Glehen O, *Cytoreductive Surgery and Peritonectomy Procedures.* Indian journal of surgical oncology, 2016. **7**(2): p. 139-151.
53. Verwaal VJ, van Ruth S, de Bree E, van Sloothen GW, van Tinteren H, Boot H, and Zoetmulder FA, *Randomized trial of cytoreduction and hyperthermic intraperitoneal chemotherapy versus systemic chemotherapy and palliative surgery in patients with peritoneal carcinomatosis of colorectal cancer.* J Clin Oncol, 2003. **21**(20): p. 3737-43.
54. Elias D, Lefevre JH, Chevalier J, Brouquet A, Marchal F, Classe JM, Ferron G, Guilloit JM, Meeus P, Goéré D, and Bonastre J, *Complete cytoreductive surgery plus intraperitoneal chemohyperthermia with oxaliplatin for peritoneal carcinomatosis of colorectal origin.* J Clin Oncol, 2009. **27**(5): p. 681-5.
55. Yan TD, Deraco M, Baratti D, Kusamura S, Elias D, Glehen O, Gilly FN, Levine EA, Shen P, Mohamed F, Moran BJ, Morris DL, Chua TC, Piso P, and Sugarbaker PH, *Cytoreductive surgery and hyperthermic intraperitoneal chemotherapy for malignant peritoneal mesothelioma: multi-institutional experience.* J Clin Oncol, 2009. **27**(36): p. 6237-42.
56. Sugarbaker PH, *New standard of care for appendiceal epithelial neoplasms and*

pseudomyxoma peritonei syndrome? Lancet Oncol, 2006. **7**(1): p. 69-76.

57. Morgan RJ, Synold TW, Xi B, Lim D, Shibata S, Margolin K, Schwarz RE, Leong L, Somlo G, Twardowski P, Yen Y, Chow W, Tetef M, Lin P, Paz B, Koczywas M, Wagman L, Chu D, Frankel P, Stalter S, and Doroshow JH, *Phase I Trial of Intraperitoneal Gemcitabine in the Treatment of Advanced Malignancies Primarily Confined to the Peritoneal Cavity.* Clinical Cancer Research, 2007. **13**(4): p. 1232.
58. Sugarbaker PH, Graves T, DeBruijn EA, Cunliffe WJ, Mullins RE, Hull WE, Oliff L, and Schlag P, *Early postoperative intraperitoneal chemotherapy as an adjuvant therapy to surgery for peritoneal carcinomatosis from gastrointestinal cancer: pharmacological studies.* Cancer Res, 1990. **50**(18): p. 5790-4.
59. Elias D, Benizri E, Di Pietrantonio D, Menegon P, Malka D, and Raynard B, *Comparison of Two Kinds of Intraperitoneal Chemotherapy Following Complete Cytoreductive Surgery of Colorectal Peritoneal Carcinomatosis.* Annals of Surgical Oncology, 2007. **14**(2): p. 509-514.
60. Topuz E, Saip P, Aydiner A, Salihoglu Y, Aydin Y, and Topuzlu C, *Catheter complications associated with intraperitoneal chemotherapy.* European journal of gynaecological oncology, 1998. **19**(3): p. 275-279.
61. Sugarbaker P, *Technical Handbook for the Integration of Cytoreductive Surgery and*

Perioperative Intraperitoneal Chemotherapy into the Surgical Management of Gastrointestinal and Gynecologic Malignancy. 4 ed. Grand Rapids. 2005, Michigan, USA: Ludann Company. p. 1-67.

62. Nadiradze G, Horvath P, Sautkin Y, Archid R, Weinreich F-J, Königsrainer A, and Reymond MA, *Overcoming Drug Resistance by Taking Advantage of Physical Principles: Pressurized Intraperitoneal Aerosol Chemotherapy (PIPAC).* Cancers, 2019. **12**(1): p. 34.
63. Furman MJ, Picotte RJ, Wante MJ, Rajeshkumar BR, Whalen GF, and Lambert LA, *Higher flow rates improve heating during hyperthermic intraperitoneal chemoperfusion.* J Surg Oncol, 2014. **110**(8): p. 970-5.
64. Davigo A, Passot G, Vassal O, Bost M, Tavernier C, Decullier E, Bakrin N, Alyami M, Bonnet JM, Louzier V, Paquet C, Allaouchiche B, Glehen O, and Kepenekian V, *PIPAC versus HIPEC: cisplatin spatial distribution and diffusion in a swine model.* Int J Hyperthermia, 2020. **37**(1): p. 144-150.
65. Spiliotis J, Halkia E, Lianos E, Kalantzi N, Grivas A, Efstathiou E, and Giassas S, *Cytoreductive surgery and HIPEC in recurrent epithelial ovarian cancer: a prospective randomized phase III study.* Ann Surg Oncol, 2015. **22**(5): p. 1570-5.
66. Quénet F, Elias D, Roca L, Goéré D, Ghouti L, Pocard M, Facy O, Arvieux C, Lorimier G, Pezet

D, Marchal F, Loi V, Meeus P, Juzyna B, de Forges H, Paineau J, and Glehen O, *Cytoreductive surgery plus hyperthermic intraperitoneal chemotherapy versus cytoreductive surgery alone for colorectal peritoneal metastases (PRODIGE 7): a multicentre, randomised, open-label, phase 3 trial.* Lancet Oncol, 2021. **22**(2): p. 256-266.

67. Solass W, Kerb R, Mürdter T, Giger-Pabst U, Strumberg D, Tempfer C, Zieren J, Schwab M, and Reymond MA, *Intraperitoneal chemotherapy of peritoneal carcinomatosis using pressurized aerosol as an alternative to liquid solution: first evidence for efficacy.* Annals of surgical oncology, 2014. **21**(2): p. 553-559.
68. Solaß W, Hetzel A, Nadiradze G, Sagynaliev E, and Reymond MA, *Description of a novel approach for intraperitoneal drug delivery and the related device.* Surg Endosc, 2012. **26**(7): p. 1849-55.
69. Giger-Pabst U, Bucur P, Roger S, Falkenstein TA, Tabchouri N, Le Pape A, Lerondel S, Demtröder C, Salamé E, and Ouaissi M, *Comparison of Tissue and Blood Concentrations of Oxaliplatin Administrated by Different Modalities of Intraperitoneal Chemotherapy.* Annals of Surgical Oncology, 2019. **26**(13): p. 4445-4451.
70. Bodner G and Pardue H, *The properties of gases*, in *Chemistry: An Experimental Science*

(Bodner, George M.; Pardue, Harry L.). 1989, John Wiley & Sons: New York. p. 468.

71. Gurskii I, *Molercular Physics. Thermal Phenomena*, in *Elementary Physics. Problems and Solutions*. 1987, Mir Publishers: The Union of Soviet Socialist Republics. p. 196-197.
72. Esquis P, Consolo D, Magnin G, Pointaire P, Moretto P, Ynsa MD, Beltramo JL, Drogoul C, Simonet M, Benoit L, Rat P, and Chauffert B, *High intra-abdominal pressure enhances the penetration and antitumor effect of intraperitoneal cisplatin on experimental peritoneal carcinomatosis.* Ann Surg, 2006. **244**(1): p. 106-12.
73. Struller F, Horvath P, Solass W, Weinreich F-J, Strumberg D, Kokkalis MK, Fischer I, Meisner C, Königsrainer A, and Reymond MA, *Pressurized intraperitoneal aerosol chemotherapy with low-dose cisplatin and doxorubicin (PIPAC C/D) in patients with gastric cancer and peritoneal metastasis: a phase II study.* Therapeutic advances in medical oncology, 2019. **11**: p. 1758835919846402-1758835919846402.
74. Eveno C, Jouvin I, and Pocard M, *PIPAC EstoK 01: Pressurized IntraPeritoneal Aerosol Chemotherapy with cisplatin and doxorubicin (PIPAC C/D) in gastric peritoneal metastasis: a randomized and multicenter phase II study.* Pleura and peritoneum, 2018. **3**(2): p. 20180116-20180116.

75. Struller F, Horvath P, Solass W, Weinreich FJ, Strumberg D, Kokkalis MK, Fischer I, Meisner C, Königsrainer A, and Reymond MA, *Pressurized intraperitoneal aerosol chemotherapy with low-dose cisplatin and doxorubicin (PIPAC C/D) in patients with gastric cancer and peritoneal metastasis: a phase II study.* Ther Adv Med Oncol, 2019. **11**: p. 1758835919846402.
76. Tempfer CB, Giger-Pabst U, Seebacher V, Petersen M, Dogan A, and Rezniczek GA, *A phase I, single-arm, open-label, dose escalation study of intraperitoneal cisplatin and doxorubicin in patients with recurrent ovarian cancer and peritoneal carcinomatosis.* Gynecol Oncol, 2018. **150**(1): p. 23-30.
77. Kurtz F, Struller F, Horvath P, Solass W, Bösmüller H, Königsrainer A, and Reymond MA, *Feasibility, Safety, and Efficacy of Pressurized Intraperitoneal Aerosol Chemotherapy (PIPAC) for Peritoneal Metastasis: A Registry Study.* Gastroenterology research and practice, 2018. **2018**: p. 2743985-2743985.
78. Gockel I, Jansen-Winkeln B, Haase L, Niebisch S, Moulla Y, Lyros O, Lordick F, Schierle K, Wittekind C, and Thieme R, *Pressurized IntraPeritoneal Aerosol Chemotherapy (PIPAC) in patients with peritoneal metastasized colorectal, appendiceal and small bowel cancer.* Tumori, 2020. **106**(1): p. 70-78.
79. Tempfer CB, Winnekendonk G, Solass W, Horvat R, Giger-Pabst U, Zieren J, Rezniczek GA,

and Reymond MA, *Pressurized intraperitoneal aerosol chemotherapy in women with recurrent ovarian cancer: A phase 2 study.* Gynecol Oncol, 2015. **137**(2): p. 223-8.

80. Giger-Pabst U, Demtröder C, Falkenstein TA, Ouaissi M, Götze TO, Rezniczek GA, and Tempfer CB, *Pressurized IntraPeritoneal Aerosol Chemotherapy (PIPAC) for the treatment of malignant mesothelioma.* BMC Cancer, 2018. **18**(1): p. 442.
81. Di Giorgio A, Abatini C, Attalla El Halabieh M, Vita E, Vizzielli G, Gallotta V, Pacelli F, and Rotolo S, *From palliation to cure: PIPAC for peritoneal malignancies.* Minerva Med, 2019. **110**(4): p. 385-398.
82. Khosrawipour V, Khosrawipour T, Kern AJ, Osma A, Kabakci B, Diaz-Carballo D, Förster E, Zieren J, and Fakhrian K, *Distribution pattern and penetration depth of doxorubicin after pressurized intraperitoneal aerosol chemotherapy (PIPAC) in a postmortem swine model.* J Cancer Res Clin Oncol, 2016. **142**(11): p. 2275-80.
83. Kakchekeeva T, Demtröder C, Herath NI, Griffiths D, Torkington J, Solaß W, Dutreix M, and Reymond MA, *In Vivo Feasibility of Electrostatic Precipitation as an Adjunct to Pressurized Intraperitoneal Aerosol Chemotherapy (ePIPAC).* Ann Surg Oncol, 2016. **23**(Suppl 5): p. 592-598.

84. Reymond M, Demtroeder C, Solass W, Winnekendonk G, and Tempfer C, *Electrostatic precipitation Pressurized IntraPeritoneal Aerosol Chemotherapy (ePIPAC): first in-human application.* Pleura Peritoneum, 2016. **1**(2): p. 109-116.
85. Graversen M, Detlefsen S, Ellebaek SB, Fristrup C, Pfeiffer P, and Mortensen MB, *Pressurized IntraPeritoneal Aerosol Chemotherapy with one minute of electrostatic precipitation (ePIPAC) is feasible, but the histological tumor response in peritoneal metastasis is insufficient.* Eur J Surg Oncol, 2020. **46**(1): p. 155-159.
86. Taibi A, Teixeira Farinha H, Durand Fontanier S, Sayedalamin Z, Hübner M, and Sgarbura O, *Pressurized Intraperitoneal Aerosol Chemotherapy Enhanced by Electrostatic Precipitation (ePIPAC) for Patients with Peritoneal Metastases.* Ann Surg Oncol, 2020.
87. Tsong TY, *Electroporation of cell membranes.* Biophysical journal, 1991. **60**(2): p. 297-306.
88. Mir LM, Orlowski S, Belehradek J, Jr., and Paoletti C, *Electrochemotherapy potentiation of antitumour effect of bleomycin by local electric pulses.* Eur J Cancer, 1991. **27**(1): p. 68-72.
89. Belehradek M, Domenge C, Luboinski B, Orlowski S, Belehradek J, Jr., and Mir LM, *Electrochemotherapy, a new antitumor treatment. First clinical phase I-II trial.* Cancer, 1993. **72**(12): p. 3694-700.

90. Glass LF, Jaroszeski M, Gilbert R, Reintgen DS, and Heller R, *Intralesional bleomycin-mediated electrochemotherapy in 20 patients with basal cell carcinoma.* J Am Acad Dermatol, 1997. **37**(4): p. 596-9.
91. *DE NOVO CLASSIFICATION REQUEST FOR ULTRAVISION™ VISUAL FIELD CLEARING SYSTEM*. [cited 21.05. 2021]; Available from: https://www.accessdata.fda.gov/cdrh_docs/reviews/DEN150022.pdf.
92. Rovers KP, Lurvink RJ, Wassenaar EC, Kootstra TJ, Scholten HJ, Tajzai R, Deenen MJ, Nederend J, Lahaye MJ, Huysentruyt C, Jr., van 't Erve I, Fijneman RJ, Constantinides A, Kranenburg O, Los M, Thijs AM, Creemers G-JM, Burger JW, Wiezer MJ, Boerma D, Nienhuijs SW, and de Hingh IH, *Repetitive electrostatic pressurised intraperitoneal aerosol chemotherapy (ePIPAC) with oxaliplatin as a palliative monotherapy for isolated unresectable colorectal peritoneal metastases: protocol of a Dutch, multicentre, open-label, single-arm, phase II study (CRC-PIPAC).* BMJ open, 2019. **9**(7): p. e030408-e030408.
93. Lurvink RJ, Tajzai R, Rovers KP, Wassenaar ECE, Moes DAR, Pluimakers G, Boerma D, Burger JWA, Nienhuijs SW, de Hingh I, and Deenen MJ, *Systemic Pharmacokinetics of Oxaliplatin After Intraperitoneal Administration by Electrostatic Pressurized Intraperitoneal Aerosol Chemotherapy (ePIPAC) in Patients with*

Unresectable Colorectal Peritoneal Metastases in the CRC-PIPAC Trial. Ann Surg Oncol, 2021. **28**(1): p. 265-272.

94. *Ultravision Visual Field Clearing System. User Manual v7.0*. 2018 [cited 24.05 2021]; Available from: https://www.bowa-medical.com/tradepro/shop/artikel/allgemein/ALESI_IFU_12284_S0_ULTRAVISION_GENERATOR_ML.pdf.
95. Lurvink RJ, Rauwerdink P, Rovers KP, Wassenaar ECE, Deenen MJ, Nederend J, Huysentruyt CJR, van 't Erve I, Fijneman RJA, van der Hoeven E, Seldenrijk CA, Constantinides A, Kranenburg O, Los M, Herbschleb KH, Thijs AMJ, Creemers GM, Burger JWA, Wiezer MJ, Nienhuijs SW, Boerma D, and de Hingh I, *First-line palliative systemic therapy alternated with electrostatic pressurised intraperitoneal aerosol chemotherapy (oxaliplatin) for isolated unresectable colorectal peritoneal metastases: protocol of a multicentre, single-arm, phase II study (CRC-PIPAC-II).* BMJ Open, 2021. **11**(3): p. e044811.
96. *Guideline on the quality requirements for drug-device combinations*. [cited 03.05.2021]; Available from: https://www.ema.europa.eu/en/documents/scientific-guideline/draft-guideline-quality-requirements-drug-device-combinations_en.pdf.

97. *Obtained from Metecon GmbH, Mannheim, Germany on 28.04.2021*.
98. *Regulation (EU) 2017/745 of the European Parliament and of the Council of 5 April 2017 on medical devices, amending Directive 2001/83/EC, Regulation (EC) No 178/2002 and Regulation (EC) No 1223/2009 and repealing Council Directives 90/385/EEC and 93/42/EEC (Text with EEA relevance.)*. [cited 03.05.2021]; Available from: https://www.medical-device-regulation.eu/download-mdr/.
99. Steuperaert M, Debbaut C, Segers P, and Ceelen W, *Modelling drug transport during intraperitoneal chemotherapy.* Pleura Peritoneum, 2017. **2**(2): p. 73-83.
100. Yu LX, Amidon G, Khan MA, Hoag SW, Polli J, Raju GK, and Woodcock J, *Understanding pharmaceutical quality by design.* Aaps j, 2014. **16**(4): p. 771-83.
101. *ICH Q8 (R2) Pharmaceutical development*. [cited 30.04.2021]; Available from: https://www.ema.europa.eu/en/ich-q8-r2-pharmaceutical-development.
102. Ter Horst JP, Turimella SL, Metsers F, and Zwiers A, *Implementation of Quality by Design (QbD) Principles in Regulatory Dossiers of Medicinal Products in the European Union (EU) Between 2014 and 2019.* Ther Innov Regul Sci, 2021. **55**(3): p. 583-590.
103. Jameel F, Hershenson S, Khan MA, and Martin-Moe S. *Quality by Design for Biopharmaceutical*

Drug Product Development. in *AAPS Advances in the Pharmaceutical Sciences Series*. 2015.

104. *ISSPP CONGRESS 2022 3RD CONGRESS OF THE INTERNATIONAL SOCIETY FOR THE STUDY OF PLEURA AND PERITONEUM.* Pleura Peritoneum, 2023. **8**(1): p. A1-a47.
105. Tidadini F, Ezanno A-C, Trilling B, Aime A, Abba J, Quesada J-L, Foote A, Chevallier T, Glehen O, Faucheron J-L, Chkair S, and Arvieux C, *Hospitalization cost of Pressurized Intraperitoneal Aerosol chemotherapy (PIPAC).* European Journal of Surgical Oncology, 2023. **49**(1): p. 165-172.
106. Sautkin I, *Development and validation of an ex vivo model for optimizing intraperitoneal drug delivery*. 2022, University of Tuebingen: Tuebingen, Germany. p. 212.
107. Orlowski S, Belehradek J, Jr., Paoletti C, and Mir LM, *Transient electropermeabilization of cells in culture. Increase of the cytotoxicity of anticancer drugs.* Biochem Pharmacol, 1988. **37**(24): p. 4727-33.
108. Burz C, Berindan-Neagoe IB, Balacescu O, Tanaselia C, Ursu M, Gog A, Vlase L, Chintoanu M, Balacescu L, Leucuta SE, Irimie A, and Cristea V, *Clinical and pharmacokinetics study of oxaliplatin in colon cancer patients.* J Gastrointestin Liver Dis, 2009. **18**(1): p. 39-43.
109. Tang HL, Tang HM, Mak KH, Hu S, Wang SS, Wong KM, Wong CS, Wu HY, Law HT, Liu K, Talbot CC, Jr., Lau WK, Montell DJ, and Fung

MC, *Cell survival, DNA damage, and oncogenic transformation after a transient and reversible apoptotic response.* Mol Biol Cell, 2012. **23**(12): p. 2240-52.

110. Rahimi-Gorji M, Debbaut C, Ghorbaniasl G, Cosyns S, Willaert W, and Ceelen W, *Optimization of intraperitoneal aerosolized drug delivery using computational fluid dynamics (CFD) modeling.* Sci Rep, 2022. **12**(1): p. 6305.
111. Eveno C, Haidara A, Ali I, Pimpie C, Mirshahi M, and Pocard M, *Experimental pharmacokinetics evaluation of chemotherapy delivery by PIPAC for colon cancer: first evidence for efficacy.* Pleura Peritoneum, 2017. **2**(2): p. 103-109.
112. Davigo A, Passot G, Vassal O, Bost M, Tavernier C, Decullier E, Bakrin N, Alyami M, Bonnet J-M, Louzier V, Paquet C, Allaouchiche B, Glehen O, and Kepenekian V, *PIPAC versus HIPEC: cisplatin spatial distribution and diffusion in a swine model.* International Journal of Hyperthermia, 2020. **37**(1): p. 144-150.

7 Own publication

ISSPP CONGRESS 2022 3RD CONGRESS OF THE INTERNATIONAL SOCIETY FOR THE STUDY OF PLEURA AND PERITONEUM. Pleura Peritoneum. 2023 Mar 29;8(1):A1-A47. doi: 10.1515/pp-2023-0010. PMID: 37020470; PMCID: PMC10067550.

8 Declaration of Contributions

In this doctoral dissertation, the following steps were performed:

- Study design:

I.Sautkin and M. Reymond proposed the study design. I. Sautkin developed the electrostatic cell culture models.

- Modeling and manufacturing of the electrostatic cell culture model:

A list of all components needed for the electrostatic cell culture model was drawn and ordered by I. Sautkin. Installation of all model components was performed by I. Sautkin.

- Laboratory experiments:

I. Sautkin conducted all experiments.

- Experiment data were collected and documented by I. Sautkin.

- Preanalytical sample preparation for measurement of drug concentration was provided by I. Sautkin and the analyses themselves were performed in an external laboratory.
- The microscopic measurements of doxorubicin tissue penetration in the Rabbit model were by I. Sautkin and A. Castagna
- Statistical calculations and data analysis were performed by I. Sautkin.
- Data gathering and analysis were performed by I. Sautkin.
- The work was supervised by M. Reymond
- The manuscript was written by I. Sautkin.
- The manuscript was reviewed by A. Königsrainer and M. Reymond
- Academic supervision was by A. Königsrainer and U. Lauer

9 Acknowledgements

I would like to thank my supervisors, Professor Marc Reymond, Professor Ulrich Lauer, and Professor Alfred Königsrainer, for a unique opportunity to join your research team and for your support and mentoring.

Furthermore, I would like to thank:

- The research team of the Department of General-, Visceral and Transplant Surgery, University Clinic Tuebingen, for the knowledge and experience I gained working with you,

- The Faculty of Medicine and Doctoral Office at the University of Tuebingen for allowing me to join the M.D. and Ph.D. program and exciting and diverse educational program.

- My academic and clinical colleagues for personal inspiration.

Finally, I would like to thank my family for their constant support and care.

10 Appendix

10.1 Physical experiments

PIPAC

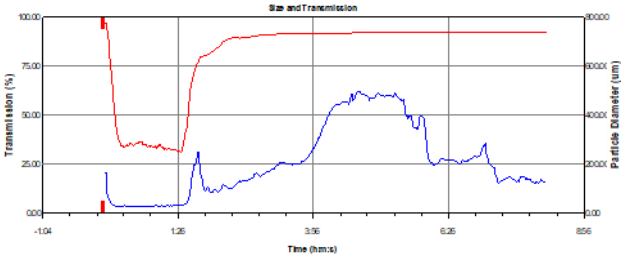

Figure 40. Measurement 2. Real-time aerosol sedimentation and transmission during PIPAC.

Real-time aerosol sedimentation (blue line) and transmission (red line). Aerosol was generated by Capnopen® from 60ml distilled water.

Figure 40 shows overtime transmission and MAD during PIPAC with distilled water. At the beginning of aerosolization, the MAD line falls and remains constant at 21.49µm for 81sec. Further, the line picks over 200µm and quickly grows above 450µm. By reaching a plateau from 259 to 340sec, the MAD stepwise declines below 200µm ending horizontally.

At the same time, transmission sharply decreases below 35% during the first 21sec following stagnation from 21 to 76sec. The line rapidly recovers over 85% by 141sec with continuous slight growth until the end of the experiment. The measurement was over 492sec.

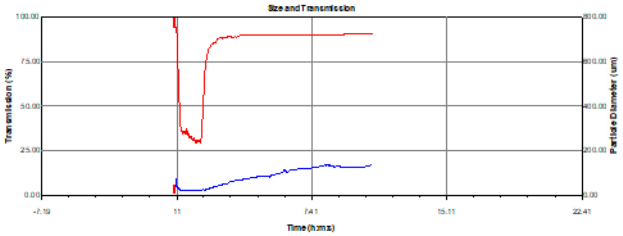

Figure 41. Measurement 3. Real-time aerosol sedimentation and transmission during PIPAC.

Real-time aerosol sedimentation (blue line) and transmission (red line). Aerosol was generated by Capnopen® from 60ml distilled water.

Measurement 3 depicts the MAD line decreasing at the beginning of aerosolization and turning into the plateau at 25.46µm for 82sec. After stagnation, the line steadily goes up for 559sec, exceeding 130µm at the end of the experiment. At the beginning of

aerosolization, the transmission line shows the same tendency as the MAD line by rapidly plummeting below 35%. However, there was no plateau. After 95sec, the transmission sharply climbs over 85%, with further recovery until the end measurement. The observation was 670sec.

ePIPAC: setup 1.

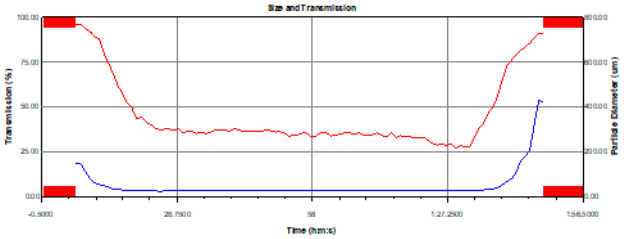

Figure 42. Measurement 2. Real-time median aerodynamic diameter and transmission during ePIPAC. Setup 1

Real-time median aerodynamic diameter (blue line) and transmission (red line). Setup 1: e-charge applied after aerosolization. Aerosol was generated by Capnopen® from 60ml distilled water.

The second measurement demonstrates a considerable MAD plunge over 7sec following stagnation at 26.71µm for 82sec and ending with a

substantial increase for 11sec over 434.2µm. The transmission steeply falls in 29sec below 35%, then moderately declines for 64sec and finally picks to 91.5%. The measurement was completed automatically by SprayTec® after 100sec due to the complete clearance of measurement space.

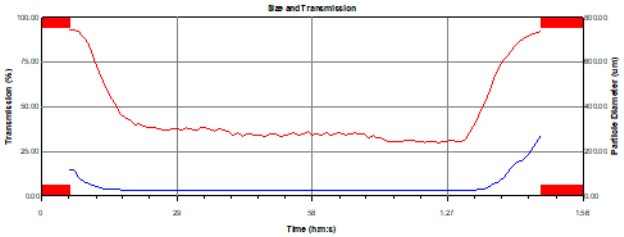

Figure 43. Measurement 3. Real-time median aerodynamic diameter and transmission during ePIPAC. Setup 1

Real-time median aerodynamic diameter (blue line) and transmission (red line). Setup 1: e-charge applied after aerosolization. Aerosol was generated by Capnopen® from 60ml distilled water.

The third measurement shows the MAD line slowly declines for 7sec, reaching a plateau at 26.68µm for 82sec and rapidly growing above 270µm in 13sec. Transmission plunges under 35% by 30sec, slowly

drops for 63sec, and further rises over 92.2%. The measurement was 102sec and finished automatically by SprayTec®.

ePIPAC: setup 2.

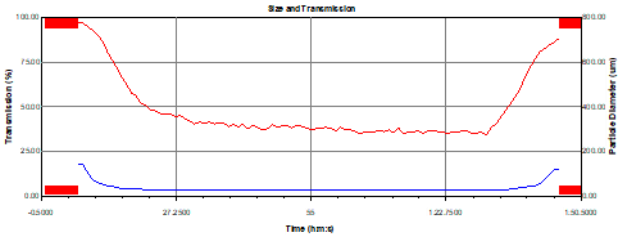

Figure 44. Measurement 2. Real-time median aerodynamic diameter and transmission during ePIPAC. Setup 2

Real-time median aerodynamic diameter (blue line) and transmission (red line). Setup 2: e-charge for the whole experiment. Aerosol was generated by Capnopen® from 60ml distilled water.

Figure 44 depicts MAD considerably decreases for 8sec, stabilises at 26.37µm for 79sec, and picks up over 100µm in 9sec. The transmission was rapidly dropping under 50% for 22sec, further declining to under 35% in 61sec and sharply going up over 85% in 15sec. The measurement was 98sec.

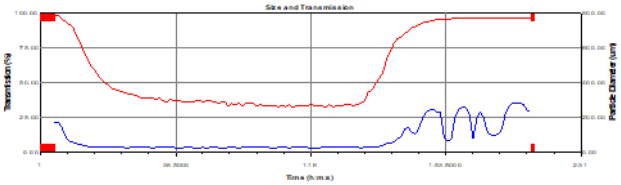

Figure 45. Measurement 3. Real-time median aerodynamic diameter and transmission during ePIPAC. Setup 2

Real-time median aerodynamic diameter (blue line) and transmission (red line). Setup 2: e-charge for the whole experiment. Aerosol was generated by Capnopen® from 60ml distilled water.

The third measurement shows MAD quickly falling for 8sec, stagnating at 26.64µm for 85sec, fluctuating for 43sec between 100-300µm and ending over 200µm. The transmission line was substantially plummeting for 26sec, gradually decreasing below 35% in 62sec and rapidly recovering over 96% in 26sec turning into the plateau for 22sec. The record time was 136sec.